



**University of
Zurich^{UZH}**

The Impacts of Glaciers on Stream Biofilm Biomass – An interdisciplinary Journey into a harsh Ecosystem

GEO 511 Master's Thesis

Author

Martina Schön
13-123-971

Supervised by

Prof. Dr. Michael Zemp
Dr. Michail Styllas (michail.styllas@epfl.ch)

Faculty representative

Prof. Dr. Andreas Vieli

30.06.2021

Department of Geography, University of Zurich



Universität
Zürich^{UZH}

EPFL



THE IMPACTS OF GLACIERS ON STREAM BIOFILM BIOMASS AN INTERDISCIPLINARY JOURNEY INTO A HARSH ECOSYSTEM



GEO 511 MASTER's THESIS

Author

Martina Schön

martina.schoen@uzh.ch

13-123-971

Supervisors

Prof. Dr. Michael Zemp

michael.zemp@geo.uzh.ch

Faculty member

Prof. Dr. Andreas Vieli

andreas.vieli@geo.uzh.ch

Dr. Michail Styllas

michail.styllas@epfl.ch

June 30th 2021

Department of Geography, University of Zurich

Title photo: Skhelda glacier, Russia (Matteo Tolosano)

Acknowledgements

I will not forget the day we were sitting in my future supervisor's office and discussed a potential thesis topic involving a maximum of one or two days of fieldwork. Fortunately, things turned out very differently and I want to sincerely thank Michael Zemp for opening so many doors for me. I really appreciated his openness to collaborate across disciplinary and geographical boundaries and enjoyed the challenging and inspirational discussions. I am very grateful for his time, knowledge and continuous support.

Furthermore, my co-supervisor Michail Styllas greatly deserves my gratitude. He helped me climbing the ups and downs of this process, translated between glaciology and stream ecology and provided me with helpful feedback. I got to enjoy many discussions with him throughout the project, at the four corners of the world and sometimes despite high altitude slowing down our brains. I further want to thank him for planning the field campaigns and tackling nerve-wracking logistical challenges with humor, as well as endurance.

My faculty member Andreas Vieli not only inspired me in terms of glaciology, but also lit a spark of curiosity in me to experience Greenland. I'm very grateful for his decisive feedback on my thesis concept and for giving me the freedom to dive into stream ecology.

I want to thank Tom Battin for allowing me to find a balance between my work as a technician and my master thesis. I appreciated our insightful exchanges on stream ecology no matter whether in the office, online or somewhere in the middle of the Nepalese nowhere. Many thanks to him and to the NOMIS foundation for enabling me to work in these fascinating places.

Special thanks go to Matthias Huss for sharing his modelling data and providing helpful explanations.

I'm very grateful for countless days in the mountains with the other field team members Matteo Tolosano and Vincent De Staercke. Together we experienced memorable scrambles, stream crossings and other ways to get soaked, as well as lots of sunshine. I want to thank them for their hands-on and moral support and for still being able to laugh together after more than nine months in the field. The same holds for all the local partners regarding their priceless help in making the travels and fieldwork happen and for spicing it up with all kinds of intercultural learnings and precious memories.

Hannes Peter, Tyler Kohler, Nic Deluigi, Leïla Ezzat and other colleagues patiently answered ecology-, R-, GIS-, or language questions and gave me valuable, as well as entertaining feedback. I want to thank them for many fruitful discussions, their pleasant company and highly welcome coffees.

Additional thanks go to Marta Boix Canadell and Urs Jakob for their well appreciated graphical support and lots of motivation.

Last but not least I'm deeply grateful to my housemates and other friends for being around and listening. The same holds for my family, with special thanks for the unconditional support I've received during all these years.

Thank you, qujanaq, spaciba, gracias, danke, takk, dhanyabad, merci!

Summary

Algae are inherent components of phototrophic biofilms and contribute to a large degree to their biomass. Biofilms form the basis of the food web and drive crucial processes in stream ecosystems. In the near future, glacier-fed streams are expected to be heavily altered by the effects of global climate change. For this reason, a better understanding of the impacts of glaciers on biofilm biomass and on the complex ecological interactions in these harsh ecosystems is needed. In this study, GIS-derived and modelled glaciological variables were combined with *in situ* measurements of physicochemical stream variables and measurements of chlorophyll a from 20 glacier-fed streams around the world. The ability of these variables to predict chlorophyll a concentration, a proxy for algal biomass, was evaluated using simple- and multivariate linear regression approaches. The variables were chosen on the basis of ecological hypotheses and are related to the glacierization of the catchment, the deglaciation time of the respective sampling points, the modelled discharge and the physicochemical properties of the streams. In a second step, their predictive power was compared with a previously established index of glacier impact on downstream ecosystems, the Glacial Index.

Of all the variables tested, the Glacial Index showed the weakest performance in predicting chlorophyll a. The poor correlation between those two variables is not in agreement with the results of a previous study and should therefore be tested again using a larger dataset with near global coverage. However, both studies agree that chlorophyll a concentration can be better explained through streamwater turbidity, the only single variable in this study capable of explaining parts of the chlorophyll a variability on a statistically significant level. Based on the results of multivariate regression modelling applied here, additional influential variables include temperature, glacier surface area and the glacier coverage of the catchment. However, multi-component models were not performing considerably better than turbidity alone and hence, this variable explains the observed variation in chlorophyll a in the most parsimonious way. Furthermore, the correlation between turbidity and chlorophyll showed a threshold behavior at approximately 250 NTU. Above this threshold, limited light availability and its impact on photosynthesis, as well as increased scouring (erosion of the biofilms) due to high sediment loads potentially inhibit the growth and survival of the algae. This threshold might represent an exciting finding but needs to be further explored using a more representative dataset. Turbidity certainly acts as a surrogate for multiple processes affecting biofilms in these inherently complex ecosystems. Increasing the range of selected variables represented in the study's dataset and reducing the uncertainties related to the glacier-fed stream complexity could potentially lead to stronger correlations between chlorophyll a and the input variables. Overall, this work indicates that glaciers exhibit a dominant control on algal biomass in glacier-fed streams. Ecological hypotheses that up to now were tentatively assumed to be valid, were quantitatively tested with identically collected data from glacier-fed streams spanning the European Alps, New Zealand, Greenland, Russia, Ecuador and Norway.

Table of Contents

Acknowledgements.....	i
Summary	iii
Table of Contents	iv
List of Abbreviations	vi
List of Figures	vii
List of Photos.....	viii
List of Tables	viii
1 Introduction.....	1
1.1 Motivation	1
1.2 Aims and research questions.....	3
2 Theoretical Background	4
2.1 Stream biofilm and chlorophyll a as proxy for algal biomass	4
2.2 Hydrological and physicochemical characteristics of glacier-fed streams	5
2.3 The habitat template of biofilm in glacier-fed streams	6
3 Study Design.....	9
3.1 Selected glaciers	9
3.2 Sampling design	11
3.3 Variable selection based on ecological hypotheses	11
4 Data and Methods.....	13
4.1 Calculation of the glaciological variables related to area and length	13
4.1.1 Data.....	13
4.1.2 GIS Analysis	15
4.1.3 Uncertainty assessment.....	18
4.2 Deglaciation analysis.....	19
4.2.1 Additional data	19
4.2.2 Reconstruction of the time of deglaciation	20
4.3 Discharge estimations	22
4.3.1 Modelling data	22
4.3.2 Calculation of the discharge variables.....	22
4.4 Fieldwork	23
4.4.1 Sediment sampling and analysis of chlorophyll a	23
4.4.2 Measurements of physicochemical stream variables.....	23
4.5 Statistical analysis.....	25
4.5.1 Detection and handling of outliers	25
4.5.2 Model choice and assessment of the dataset's statistical power	26

4.5.3	Testing the model assumptions	26
4.5.4	Variable selection	28
5	Results	30
5.1	Summary of the variables and underlying hypotheses	30
5.2	Visualization of the individual glaciological and physicochemical variables.....	32
5.2.1	Glacier area and length variables	32
5.2.2	Deglacierization of the sampling locations	33
5.2.3	Discharge estimations	33
5.2.4	Physicochemical stream variables.....	34
5.3	Observed values of chlorophyll <i>a</i>	35
5.4	Performance of the Glacial Index in predicting chlorophyll <i>a</i>	35
5.5	Correlation of the model variables with chlorophyll <i>a</i>	36
5.5.1	Simple linear regression	36
5.5.2	Multivariate linear regression	37
5.6	Potential threshold in turbidity controlling chlorophyll <i>a</i>	38
6	Discussion	39
6.1	Performance of the Glacial Index and potential alternatives to predict chlorophyll <i>a</i>	39
6.2	Interpretation of the observed threshold in turbidity	42
6.3	Limitations and potential improvements of the research design	43
7	Conclusions and Outlook	47
8	References	48
	Appendix.....	I
A.	Methods	I
B.	Results	V
	Personal Declaration	IX

List of Abbreviations

ASTER	Advanced Spaceborne Thermal Emission and Reflection Radiometer
AT	Austria
CH	Switzerland
Chl a	Chlorophyll a
CV	Coefficient of Variation
DD	Decimal Degrees
DEM	Digital Elevation Model
DM	Dry mass
DN-site	Lower sampling site
EC	Ecuador
GFS	Glacier-fed stream
GIS	Geographical Information System
GL	Greenland
GLIMS	Global Land Ice Measurements from Space
GloGEM	Global Glacier Evolution Model
GPS	Global Positioning System
NO	Norway
NTU	Nephelometric turbidity units
NZ	New Zealand
Q_{abs}	Absolute discharge
Q_{spec}	Specific discharge
R^2	Coefficient of Determination
RGI	Randolph Glacier Inventory
RU	Russia
swisstopo	Swiss Federal Office of Topography
UP-site	Upper sampling site
WGMS	World Glacier Monitoring Service
$\mu S/cm$	Microsiemens per centimeter

List of Figures

Figure 1 Scheme of algae performing photosynthesis.	5
Figure 2 Windows of opportunity for biofilm accrual in the physicochemical habitat template of glacier-fed streams in the Alps.	8
Figure 3 Already completed and planned sampling destinations of the Vanishing Glaciers project.	9
Figure 4 Remotely sensed glaciological regression variables at the example of Silvretta glacier (CH).	15
Figure 5 UP- and DN-catchments and maximal vs. minimal glacier surface area polygons at the example of Silvretta Glacier, CH.	17
Figure 6 Known glacier extents of the Tsidjoure Nouve Glacier, Switzerland, based on different data sources.	20
Figure 7 Decision tree for the deglaciation analysis. Depending on the available data sources the reconstruction was performed using method A, B, or C.	21
Figure 8 Multicollinearity before and after removing regression variables based on their variance inflation factors.	27
Figure 9 Suggested seven models containing the seven remaining variables after the procedure of strictly removing the variable with the highest VIF, until no variables with VIF > 3 were left	28
Figure 10 Assessment of the best models according to three model performance metrics.	28
Figure 11 Summary statistics for the 4-variable model.	28
Figure 12 Visualization of the spread in observations for the regression inputs surface area, glacier coverage, snout distance and Glacial Index.	32
Figure 13 Distribution of the estimated amount of years the upper and lower sampling sites have been free of ice.	33
Figure 14 Distribution of A) the total absolute discharge of the sampling month and B) the annual coefficient of variation of the monthly absolute discharge.	34
Figure 15 Distribution of measured values of A) temperature, B) turbidity and C) conductivity.	34
Figure 16 Inter- and intra-site distribution of observed chlorophyll a values.	35
Figure 17 Performance of the Glacial Index in predicting chlorophyll a using A) log-transformed B) and raw data.	35
Figure 18 Performance of 11 simple linear models in predicting chlorophyll a, sorted by Pearson correlation coefficient.	36
Figure 19 Correlation between turbidity and chlorophyll a using A) log-transformed B) and non-transformed data.	36
Figure 20 Potential turbidity threshold of approximately 250 NTU controlling chlorophyll a concentration.	38
Figure 21 A) UP- to DN-site differences in temperature and B) temperatures at UP-vs. DN sites.	44
Figure 22 UP- to DN- site differences in turbidity and B) UP- vs. DN-site turbidity levels.	45

List of Photos

Photos 1 Stream biofilms of different morphologies growing in contrasting hydraulic regimes on boulders within 50 m proximity of the snout of Storjuvbreen Glacier, NO.	4
Photos 2 Sediment sampling and measurement of physicochemical stream variables.	24
Photo 3 Heavily vegetated stream banks at the DN-site of Forno Glacier (CH).....	25
Photos 4 Visual examples of turbidities of nearly 250 NTU: A) At the UP-site of Schwarzberg Glacier (CH) 206 NTU and B) at the DN-site of Chamberlin Glacier (GL) 228 NTU were measured.	42
Photo 5 A sampling site on the Cotopaxi Volcano (EC, with similar characteristics like the stream of Antizana 15a), illustrating the pronounced differences in geological setting and topography, i.e. compared to the to the European Alps.	45

List of Tables

Table 1 The selected 20 glaciers with respective geographical characteristics and observation data availability (time period and number of observations within that period).	10
Table 2 Selected glaciological and physicochemical variables as inputs for multivariate regression.	12
Table 3 Overview of the data sources for the calculation of the glaciological variables related to area and length.	13
Table 4 Supplementary data sources used for deglaciation analysis.	19
Table 5 Glacier variables with their hypothesized effect on chlorophyll a.	30
Table 6 Physicochemical streamwater variables with their hypothesized effect on chlorophyll a.	31
Table 7 Best multivariate regression models explaining variation in chlorophyll a.	37
Table 8 Additional multivariate regression models explaining variation in chlorophyll a, based on less strict selection criteria	37

1 Introduction

1.1 Motivation

Glacier-fed streams (GFS) are heavily impacted by the effects of global climate change (Milner and others, 2017), yet we know very little about these relatively pristine and remote ecosystems (Wilhelm and others, 2013; Battin and others, 2016). Particularly little is known about the microbial life in these streams, which is dominated by complex microbial communities embedded in a self-excreted matrix called ‘biofilms’ (Battin and others, 2016). Biofilms are critical components of stream ecosystems as they form the basis of the food web, drive crucial ecosystem processes and thereby potentially impact downstream biodiversity and biogeochemistry (Battin and others, 2016). By degrading organic matter they emit a large amount of CO₂ into the atmosphere and have therefore been recognized as substantial contributors to global carbon fluxes (Battin and others, 2016). Given their important functions within the ecosystem and for downstream locations, it is crucial to deepen our understanding of the effects of climate change on these communities (Wilhelm and others, 2013).

The project ‘Vanishing Glaciers – What Else Besides Water Is Lost?’ of the Stream Biofilm and Ecosystem Research Laboratory (SBER) at École Polytechnique Fédérale de Lausanne (EPFL) aims at characterizing the microbial diversity of glacier-fed stream biofilms on a global scale while such a survey is still possible. The overall goal is to unravel the diversity and evolution of the microbes inhabiting the glacier-fed streams and to assess the impacts of climate change on biogeochemical fluxes in glacier-fed streams. As a contribution to the objectives of the project, this thesis cuts across the boundaries of glaciology and stream ecology and investigates how different glaciological and physicochemical stream variables relate to the biomass of phototrophic biofilms in glacier-fed streams.

Previous studies suggest that community assembly of microbial biofilms is not a random process but depends largely on environmental conditions (Battin and others, 2016; Besemer and others, 2012; Wilhelm and others, 2013). Biofilms in glacier-fed streams live in a habitat which has long been considered inhospitable for life due to low stream water temperatures, nutrient scarcity, high levels of turbidity, high suspended sediment loads, and strong diel and seasonal variability of discharge associated with low sediment stability (Ward, 1994; Uehlinger and others, 2010). In work on macroinvertebrates, relatively simple measures of glacial influence such as the distance to the glacier snout, relative contribution of glacier meltwater and percentage of glacier cover in the catchment have been successfully applied (reviewed in Jacobsen and Dangles, 2012). However, despite the tight ecohydrological coupling between glaciers and glacier-fed streams (Wilhelm and others, 2013), very little is known about the impact of glaciers on the biofilm habitat, or in other words, which of the above mentioned aspects exert strong controls on the biofilm living conditions in glacier-fed streams.

As an integrative proxy for the glacial influence on the stream environmental conditions, Jacobsen and Dangles (2012) formulated the Glacial Index (GI), combining glacier size with distance from the snout:

$$\text{Glacial Index (GI)} = \frac{\sqrt{\text{glacier surface area (km}^2\text{)}}}{\text{distance from snout (km)} + \sqrt{\text{glacier surface area (km}^2\text{)}}}$$

At Glacial Index = 1, the glacial influence is at its maximum (zero distance from the glacier snout) and decreases with increasing distance from the glacier. Moreover, the Glacial Index diminishes faster in

1 Introduction

streams draining from small glaciers than in streams draining from larger glaciers. Since key glaciological processes depend on glacier size, the Glacial Index integrates the effects of variables such as stream water turbidity, suspended solids and substrate type (Jacobsen and Dangles, 2012). The authors tested the explicative power of this index on taxon richness of macroinvertebrates, hypothesizing that the environmental harshness of a specific stream site highly depends on its distance from the glacier snout and the size of the glacier delivering the meltwater. In their global study, they discovered that macroinvertebrate taxon richness decreased exponentially with increased Glacial Index and they stress the advantage of the index in allowing to decouple environmental harshness from latitudinal and elevational gradients. Hence, the Glacial Index can be used as a simple and useful measure of environmental harshness in glacier-fed streams. The authors suggest it as a monitoring instrument for future and ongoing long-term studies on the effects of glacial retreat (Jacobsen and Dangles, 2012).

Following these recommendations, Lencioni (2018) used the Glacial Index for the same purpose in a study in the Alps, where it performed as one of the most robust predictors of macroinvertebrate taxon richness. Jacobsen and Dangles (2012) and Lencioni (2018) have also applied the Glacial Index to approximate unknown percentages of catchment glacier coverage from a relationship between the glacier coverage of catchments and respective Glacial Index values established by Jacobsen and others (2012).

Unlike the popular Glaciation Index by Ilg and Castella (2006), the Glacial Index does not require quantifying sediment stability based on Pfankuch scores (Pfankuch, 1975) and hence appears simpler and more objective. Benefitting from this advantage, in Kohler and others (2020, the first Vanishing Glaciers project publication) the Glacial Index was for the first time applied to biofilm biomass. The underlying argumentation was the hypothesis that the sampling point distance from the glacier and the glacier surface area will effectively determine many of the influential components of the habitat template of stream biofilms. By studying 20 glacier-fed streams in New Zealand, we found that the concentration of chlorophyll a as a proxy for algal biofilm biomass decreased with increasing Glacial Index (Kohler and others, 2020).

Thus, the Glacial Index represents one possible measure of environmental harshness. However, it is only a rough representation of glacial influence, and its value has not yet been evaluated for biofilm research on a global scale. As a consequence, current knowledge about the links between the physical characteristics of glaciers and effects on biofilm biomass in glacier-fed streams permits only vague predictions on the potential response of this habitat to climate change. This limits the potential for upscaling to larger regions and making global estimates. Milner and others (2009) and Sommaruga (2015) agree that more data on how the presence of glaciers affects algal biomass are needed, to better understand the implications of glacier retreat on primary producers.

1.2 Aims and research questions

Benefiting from the Vanishing Glaciers project database, this thesis aims to establish empirical relationships between glacier characteristics derived from remote sensing and other geographical data analyses with the biomass of phototrophic biofilms. Ultimately, the goal is to first assess the predictive power of the Glacial Index, and if necessary, make suggestions for its revision in order to better predict biofilm biomass in glacier-fed stream ecosystems.

Measurements of chlorophyll *a*, the ecologically most relevant photopigment, serve as a proxy for the biomass of eukaryotic algae and cyanobacteria, which in terms of biomass are the most abundant components of phototrophic biofilms (Battin and others, 2016). Also due to the relative simplicity of the measurement (Welschmeyer, 1994), chlorophyll *a* is often used as a proxy for algal biomass in research on freshwater ecosystems (Falkowski and Raven, 2013).

In addition to the Glacial Index, this thesis further aims to compare the predictive power of remotely-sensed variables to physicochemical variables measured in the field including turbidity, electric conductivity and water temperature. A better understanding of the relative importance of glaciological and in-stream physicochemical variables for glacier-fed stream biomass is important in order to assess the accuracy and uncertainty of upscaling exercises. Given the potential feedbacks between glacier melting and carbon cycling in glacier-fed streams, such upscaling will be important.

Regarding the glaciological (including geographical and hydrological) variables, the following aspects have been identified as the most relevant ones to be investigated:

- Characterizing the catchment above the stream sampling site regarding its absolute glacier surface area and the percentage of glacier cover
- Measuring the distance between glacier snout and stream sampling site
- Reconstructing for how long the sampling sites have been free of ice
- Estimating the total glacier contribution to the stream discharge during the sampling month, as well as the annual amplitude of the monthly total discharges

Using a multivariate linear regression approach, the relevance of glaciological variables obtained from these analyses for predicting chlorophyll *a* concentrations will be evaluated against *in situ* measured physicochemical stream variables. Consequently, the following research questions arise:

Q1: Which combination of glaciological and physicochemical stream variables possess the highest power to explain measured chlorophyll *a* values?

Q2: Should and if yes, how can the Glacial Index be revised in order to achieve a better representation of the glacial impact on stream biofilm biomass?

Even though climate change-induced rapid global glacier loss (Zemp and others, 2015, 2019; Hugonnet and others, 2021) acts as a major motivation for this research topic, this study will focus on trying to better understand the ecological interactions in the glacier-fed stream ecosystem as they are observed today.

2 Theoretical Background

2.1 Stream biofilm and chlorophyll a as proxy for algal biomass



Photos 1 Stream biofilms of different morphologies growing in contrasting hydraulic regimes on boulders within 50 m proximity of the snout of Storjuvbreen Glacier, NO.

Sediment surfaces in streams are colonized by communities of algae and heterotrophic microorganisms such as bacteria, fungi and protists (Milner and others, 2009). These microorganisms excrete an organic matrix which stabilizes these communities on the substrate (Roncoroni and others, 2019). Together, this complexes of primary producers and consumers are commonly referred to as biofilms and can be imagined as a ‘microbial skin’ covering large surfaces of the streambed (Battin and others, 2016). Life in this matrix facilitates resource capture, stimulates biotic interactions and protects its inhabitants from erosion, grazing by predators and UV radiation (Roncoroni and others, 2019). The spatial organization of microorganisms within the matrix leads to the establishment of physical and chemical gradients, which results in habitat diversity and hence, increased biodiversity (Roncoroni and others, 2019). For this reason, stream biofilms have been referred to as ‘microbial jungles’, acknowledging the fact that their diversity typically spans all three domains of life (Battin and others, 2016). Depending on the local hydraulics, they can differentiate into highly structured and diverse architectures (Photos 1), including for instance filamentous streamers, cones or microbial mats (Flemming and Wingender, 2010). Due to their role in stabilizing sediments, stream biofilms have been proposed as ‘ecosystem engineers’ (Roncoroni and others, 2019) and since species composition seems highly dependent on physicochemical habitat conditions, Wilhelm and others (2013) also termed them ‘sentinels of climate change’. Furthermore, they are hotspots of enzymatic activity, driving biochemical

cycles with important downstream implications (Battin and others, 2016). However, their major ecosystem function probably lies in gross primary production. Since the catchments of glacier-fed streams are often free of vegetation, some studies suggest that algae in biofilms are the dominant source of energy in these streams, thereby forming the base of the food web (reviewed in Uehlinger and others, 2010).

Eukaryotic algae (such as diatoms, green algae, chrysophytes, red algae and cryptophytes and cyanobacteria) are important building blocks of phototrophic biofilms and their abundance depends on the availability of light (Battin and others, 2016). Photosynthetically active radiation is absorbed by the photopigment chlorophyll a produced in algal cells. If light is available, photosynthesis can be performed and biomass is produced by metabolizing water and carbon dioxide into oxygen and organic matter (Figure 1). Due to being necessary for primary production, chlorophyll a serves as a widely used proxy to estimate algal biomass (Falkowski and Raven, 2013).

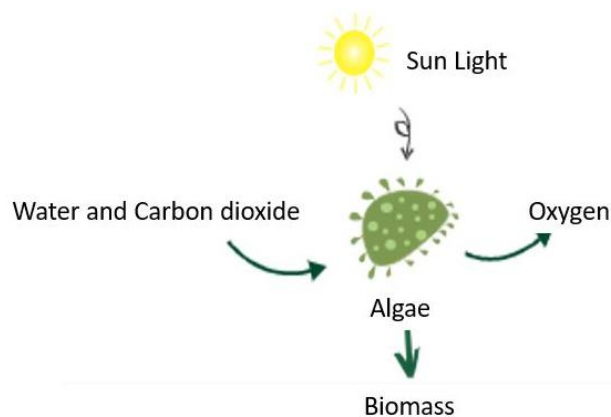


Figure 1 Scheme of algae performing photosynthesis (modified from <https://www.chegg.com/>).

2.2 Hydrological and physicochemical characteristics of glacier-fed streams

Even though the focus of this study lies on glacial meltwaters, stream flow in glacier-fed streams usually originates from multiple water sources: Ice melt, snow melt and groundwater, whose relative importance vary spatially as well as temporally (Brown and others, 2003, 2007; Milner and others, 2009). Assuming ice melt to be dominant, this section will outline some general hydrological and physicochemical characteristics of glacier-fed streams, whereas the following one will focus on their implications for the accrual and survival of stream biofilms.

Glacier-fed streams are cold ecosystems, with water temperatures near the glacier snout close to 0 °C, even during summer, but with increasing temperatures further downstream (reviewed in Brown and others, 2018). Owing to rising air temperatures from longer periods of solar radiation, maximum water temperatures are reached in May or early June at Northern hemisphere mid-latitudes (Uehlinger and others, 2003). Later in the season, this warming is counter-balanced by higher release of cold meltwater, which persistently reduces water temperatures compared to non-glacial streams at the same elevation level (Uehlinger and others, 2010). Hence, the glacier acts as a buffer and the thermal regime in glacier-fed streams can deviate substantially from the ambient temperatures (Bernhardt and others, 2018).

Typical for glacier-fed streams are their distinct and relatively predictable flow pulses (Uehlinger and others, 2003). The discharge regime is characterized by a peak in the summer dry season when non-glacial streams display low flow (Milner and others, 2009) and high temperature and radiation

2 Theoretical Background

controlled diel variations are sustained through the entire glacier melt season (reviewed in Brown and others, 2003; Uehlinger and others, 2010).

This variability in discharge contributes to the unstable character of the stream bed. Stability thereby is a function of distance from the glacier and time since deglaciation (Brown and others, 2003). With increasing distance to the glacier, streambed stability might therefore be expected to increase because variation in discharge is dampened by an increasing relative contribution of groundwater to streamwater. Longer time since deglaciation, on the other hand, may allow for sediment sorting and increased streambed stability due to a consolidation of proglacial streambeds.

Sediment transport occurs in the form of bedload carried along the channel floor, suspended load held within the flow and ions dissolved in the water (Benn and Evans, 2013). The rate of transport depends on both the availability of sediment and the characteristics of the flow, with high shear stress due to high flow velocity and discharge increasing the transport capacity (Benn and Evans, 2013).

Potential sources of sediment include supraglacial, englacial and subglacial areas (Benn and Evans, 2013). In the proglacial area, snowmelt- and rainfall-induced mass movement on ice-free slopes and lateral moraines, as well as thawing of ice-cored moraines and frozen sediments can additionally contribute to sediment supply (Łepkowska and Stachnik, 2018). The latter is primarily controlled by bedrock susceptibility to mechanical erosion in addition to glaciological variables such as basal sliding speed, glacier size, ice flux and the development of a subglacial drainage system (Łepkowska and Stachnik, 2018).

The erosive activity of glaciers releases large quantities of very fine mineral particles, typically in the size range of clays and fine silt (reviewed in Sommaruga, 2015) remaining in suspension, as long as turbulence and flow velocity are high enough relative to their specific grain size (Benn and Evans, 2013). These highly lithology-specific mineral suspensions are popularly called 'glacial flour' or 'rock flour' and are responsible for the typical 'milky' appearance of glacier-fed freshwaters (Sommaruga, 2015). This turbidity results from intense scattering of the light by the mineral particles (Davies-Colley and Smith, 2001). Stream water turbidity is an optical quantity measured in nephelometric turbidity units (NTU) and serves as a simple and cheap surrogate for measuring suspended sediment concentrations (Davies-Colley and Smith, 2001). The concentration of dissolved ions on the other hand, is estimated by measuring the electrical conductivity ($\mu\text{S}/\text{cm}$) of the stream water. The concentration of major ions (e.g. Na, Cl, K, SO_4) all contribute to streamwater electrical conductivity. These ions typically accumulate in groundwaters but high subglacial weathering rates also contribute to elevated conductivity levels (T. Kohler pers. comm.). Consequently, measured levels of electrical conductivity can vary greatly across different glacier-fed streams (Benn and Evans, 2013).

2.3 The habitat template of biofilm in glacier-fed streams

Glacier-fed streams are inherently complex and heterogeneous ecosystems (Battin and others, 2016). Not only do they drain water from multiple sources, physicochemical variables (water temperature, channel stability, suspended sediment concentration) also influence them on time-scales ranging from diel to millennial (Brown and others, 2003). This adds further complexity to the abiotic processes biofilms encounter in glacier-fed streams. In their conceptual model, Brown and others (2003) took up the challenge to visualize these complex interactions between environmental variables, as well as their impact on stream communities. It becomes very apparent that these strongly interconnected variables

should not be studied separately; nevertheless, they will be described one by one in the following paragraphs.

As a key rule of life, Brown and others (2004) state that higher temperature increases enzyme activity and metabolic rates, which results in faster growth. Their statement is based on the Boltzmann relationship and should also hold true for a moderate range of water temperature below the point where temperature becomes stressful (Elser and others, 2020). Milner and Petts (1994) agree on this temperature control on primary production caused by the effect on metabolic rates. However, some algae seem to be very specialized to cold water temperatures (Milner and others, 2009). Uehlinger and others (2010) take it one step further and state that low water temperature does not act as a primary constraint on the formation of autotrophic biofilms in glacier-fed streams.

Similarly, the effect of stream water electrical conductivity on biofilm remains unclear. This property is linked to the abundance of dissolved ions and is used as a surrogate for subglacial and stream weathering (Cano-Paoli and others, 2019). However, the specific ions are not identified and hence, it is often not clear whether specific algae can benefit from them as a source of nutrients (T. Kohler pers. comm.).

Regarding stream water turbidity, there is a strong consensus among several authors, that due to its direct effect on light availability, turbidity acts as a key constraint on autotrophic biomass production (Sommaruga, 2015; Battin and others, 2016). Light attenuates exponentially with water depth (Bernhardt and others, 2018) and the higher the concentration of sediment particles, the less light can penetrate to the stream bed and remain available for photosynthesis (Davies-Colley and Smith, 2001).

In addition to the optical impacts of stream water turbidity, high suspended sediment loads also lead to the mechanical abrasion of biofilm, termed ‘scouring’ (reviewed in Bernhardt and others, 2018). Since high bedloads cause similar disturbances, discharge is as an important factor to take into account. Floods powerful enough to mobilize bed sediments may lead to burial, scour or export of stream biofilm (Bernhardt and others, 2018). On the other hand, biofilm growth can only take place at relatively low flow velocity and streambed stability is crucial since ‘the rolling stone gathers no moss’¹, meaning that mobile substrates are unable to accumulate large quantities of biomass (Bernhardt and others, 2018)).

Cauvy-Fraunié and others (2016) conducted a study about the effects of the ‘peak water’ transition on the biomass of primary producers. ‘Peak water’ refers to the maximum annual discharge volume that is reached in a glacier-fed stream before it starts declining since the reduced glacier surface area cannot support a rising meltwater volume anymore (Huss and Hock, 2018). In a global study in 2018, Huss and Hock found that in approximately half of the studied basins, this tipping point had already passed. Regarding the effects of this transition on primary producers, the experimental flow reduction by Cauvy-Fraunié and others (2016) in an Andean glacier-fed stream was followed by a strong increase in the biomass of primary producers. In addition to lower stress owing to less turbidity and mechanical disturbance, this might also be attributed to higher water temperatures (Uehlinger and others, 2010).

¹ First recorded in 1508 by Erasmus in his collection of Latin proverbs, Adagia (Bernhardt and others, 2018).

2 Theoretical Background

Lastly, by inundating areas or letting them fall dry, discharge also controls the habitable area for stream biofilms (Bernhardt and others, 2018).

Summarizing the effects of all these variables, it comes as no surprise that seasons play an important role in the physicochemical habitat template of these streams. In the Alps, this template is characterized by distinct and predictable changes between harsh and relatively benign periods (Uehlinger and others, 2010). During so-called ‘windows of opportunity’ (Figure 2) the metabolic rates are high and due to minimal disturbance, algal biomass reaches its seasonal peak (Bernhardt and others, 2018). In glacier-fed streams, these time windows of high light availability due to reduced turbidity and lack of snow cover, as well as relatively low and stable discharge occur most-likely before and certainly at the end of the ablation season (Uehlinger and others, 2010).

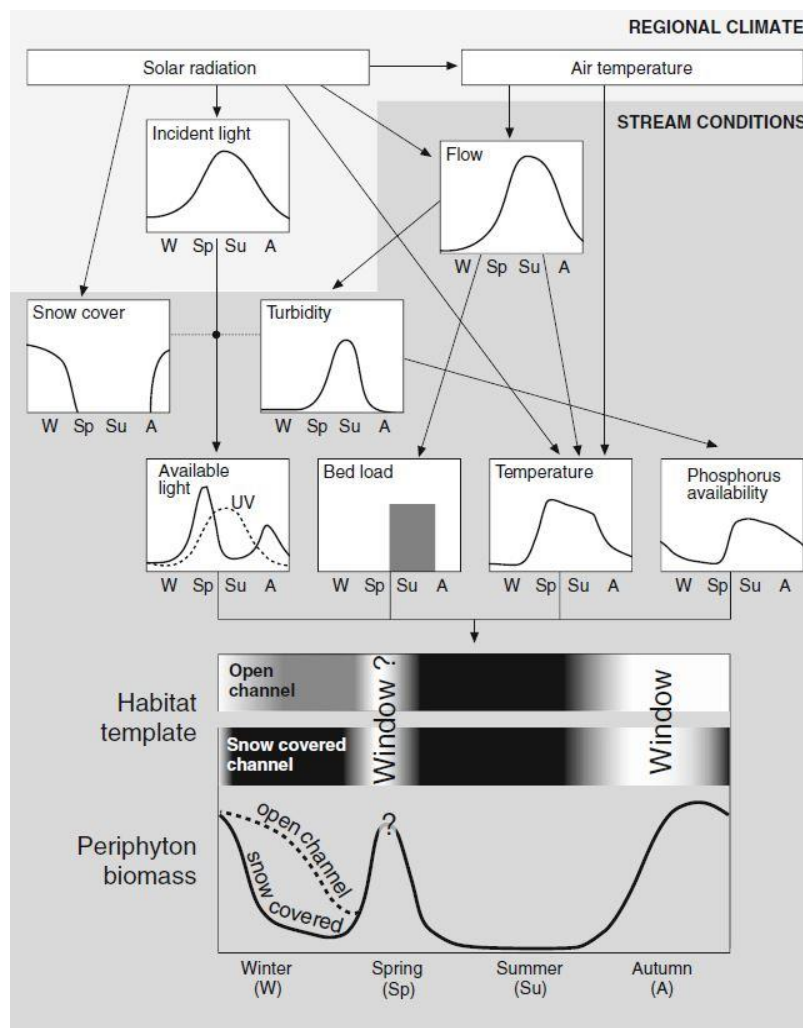


Figure 2 Windows of opportunity for biofilm accrual in the physicochemical habitat template of glacier-fed streams in the Alps (Uehlinger and others, 2010).

3 Study Design

3.1 Selected glaciers



Figure 3 Already completed and planned sampling destinations of the Vanishing Glaciers project (map produced using Esri data).

To achieve the goals of the present Master's thesis, 20 glaciers from the Vanishing Glaciers project dataset have been selected. This calls for an explanation about the original selection criteria for all the sampled 100 glaciers. Since the aim of this ongoing research project is to establish a census of the microorganisms living in glacier-fed streams on a global scale, the sampling destinations have been chosen in order to represent the major mountain ranges of the planet. The choice of these destinations is illustrated in Figure 3, distinguishing between field campaigns already completed from February 2019 to September 2020 and the remaining planned destinations.

Once a sampling destination was defined, several selection layers including logistical constraints and scientific criteria, led to the actual choice of the glaciers, or more precisely of the respective glacier-fed streams to be sampled. From a scientific point of view, it was important to choose glacier-fed streams that

- allow a safe approach and working conditions near the glacier terminus
- have discharge at the time of sampling, which originates primarily from ice- and not from snow melt
- show neither stream intermittency (i.e. water flowing below moraines), nor waterfalls that could affect sediment dynamics and stream physicochemical properties
- have no proglacial lake between the glacier snout and the stream, which could impact sediment dynamics and act as a nutrient sink
- contain adequate quantities of sediments in the medium sand grain-size range, which are favorable for the extraction of biofilm.

Due to the wide range of analyses performed for this project, equipment weight and fieldwork protocol length put some additional logistical constraints on the selection of glaciers. Among all the glaciers of one fieldwork destination that fulfilled the mentioned criteria, the final selection was done based on maximal possible diversity in climatological conditions (i.e. gradients in latitude and continentality),

3 Study Design

glacier size and orientation, as well as the availability of mass balance or front variation data from the World Glacier Monitoring Service (WGMS, 2020, and earlier reports).

While selecting 20 glaciers, priority was given to the Swiss ones, owing to the extraordinary availability of high-resolution maps and orthophotos, as well as observational data. To avoid losing the global perception of the project's samples, the Swiss selected glaciers were complemented by one glacier from each of the remaining sampled destinations (Figure 3). The selection of the non-Swiss glaciers was performed based on their WGMS glacier inventory data availability. The general geographical characteristics and available observational data for the 14 Swiss and 6 international glaciers are listed in Table 1.

Table 1 The selected 20 glaciers with respective geographical characteristics and observation data availability (time period and number of observations within that period). All geographical information stems from the WGMS Fluctuations of Glaciers Database (WGMS, 2019) and not from any GIS analysis conducted in the course of this thesis.

WGMS Glacier Name	Polit . Unit	Surface Area (km ²)	Length (km)	Snout elevation (m)	Mass Balance	# MB Obs.	Front Variation	# FV Obs
Swiss Alps								
Silvretta	CH	2.7	3.3	2475	1918-2017	99	1956-2016	57
Findelen	CH	12.9	6.9	2500	2004-2016	12	1885-2016	88
Schwarzberg	CH	5.1	4.1	2600	1955-2016	61	1880-2016	86
Forno	CH	6.2	5.8	2231	1954-1960	6	1833-2016	118
Albigna	CH	2.5	3.4	2179	1954-1960	6	1855-2015	13
Tschierva	CH	11.8	5	2340	-	-	1934-2016	70
Arolla (Bas)	CH	5.4	5.1	2168	-	-	1856-2016	122
Mont Mine	CH	9.8	5.4	2023	-	-	1956-2016	55
Roseg	CH	6.7	3.7	2197	-	-	1655-2016	110
Morteratsch	CH	14.2	7.4	2021	-	-	1874-2016	129
Tsidjore Nouve	CH	2.7	5	2289	-	-	1882-2018	125
Valsorey	CH	1.9	3.8	2440	-	-	1890-2018	119
Trift VS	CH	1.6	2.4	2813	-	-	-	-
Hohlaub-N	CH	0.3	0.9	3123	-	-	-	-
International								
Brewster	NZ	2	2.7	1676	2005-2018	14	1983-2018	34
Djankuat	RU	2.3	3.4	2738	1968-2009	52	1966-2019	34
Antizana 15α	EC	0.3	1.9	4858	1995-2018	24	1965-2017	24
Hintereisferner	AT	6.2	6.4	2450	1953-2019	67	1847-2018	125
Storbreen	NO	5.1	2.9	1400	1949-2019	71	1888-2018	85
Chamberlin	GL	7.8	3.8	370	-	-	1894-2005	9

3.2 Sampling design

Every glacier-fed stream was sampled on the same day in two locations, in order to be able to assess the glacier influence on biofilm characteristics in a downstream gradient. For this purpose, the upper site (UP-site) was chosen as close to the glacier terminus as safely possible and the lower one (DN-site) further downstream in a variable distance from the terminus (Figure 4), but before any confluence with a stream from another glacier or different water source, a lake or any kind of stream intermittency. The unique characteristics of the selected glaciers, their streams and the usually challenging terrain, make it nearly impossible to standardize the distances between the glacier snout and the sampling sites. Ultimately, these distances ranged from 2 - 331 m in the case of the UP-sites and 200 - 1402 m in the case of the DN-sites (see sub-chapter 5.2.1).

The upper sites were consistently approached and sampled first, 2.5 - 4 h before the DN-site. For the methodological approach of the thesis, the data derived from the upper and lower sampling sites, respectively, are treated as individual observations, as if they would originate from two separate glaciers. The implications of this assumption on the interpretation of results are discussed in section 6.3.

A detailed description of the fieldwork protocol follows in sub-chapter 4.4. However, it is important to emphasize that the chlorophyll a analyses were undertaken on the biofilm of the medium sand populations of the streams and do not include biofilm growing on boulders as seen in Photos 1. The main reasons for this are based on the fact that: i) sampling three random patches of bedload sediments with invisible biofilm appears more objective in relation to the hydraulic conditions and biofilm abundance and ii) it is often not possible to find boulder biofilms large enough to be sampled, especially if they grow on a rock or boulder which cannot be removed from the stream.

3.3 Variable selection based on ecological hypotheses

In order to attempt to explain the observed chlorophyll a variability, a set of regression variables was defined. A preselection was given by the analysis and measurement data available from the Vanishing Glaciers project. Based on an extensive literature review and several expert discussions, ecological hypotheses were formulated and served as the argumentative basis for the final selection of regression variables. The resulting glaciological and physicochemical variables are listed in Table 2 and are presented in detail in sub-chapter 5.1. In terms of geographical information, sampling point elevation could have served as an additional helpful proxy for environmental harshness, but had to be excluded since in terms of climatic conditions it is meaningless to compare elevation across such a large latitudinal gradient (Odum and Barrett, 2004). Similarly, stream aspect might have contributed to explaining some variation in light availability, but could not be included in the planned statistical approach as the only categorical variable among numerical ones. Additional physicochemical variables measured in the field include pH, dissolved oxygen (DO) concentration and the partial pressure of carbon dioxide ($p\text{CO}_2$). Due to the risk of encountering measurement errors in the case of pH (very delicate probes used in rough field conditions) and expected variability in DO and $p\text{CO}_2$ due to very local hydraulic conditions, these variables have not been included, either. According to the literature review and expert discussions, for none of them a direct impact on biofilm biomass has been hypothesized.

3 Study Design

Table 2 Selected glaciological and physicochemical variables as inputs for multivariate regression.

Variable name	Description	Unit
Latitude	Latitude of the sampling point	DD
Surface area	Glacier surface area	km ²
Glacier coverage	Glacier coverage of the catchment above the sampling point	%
Snout distance	Straight line distance from the glacier snout to the sampling site	m
Glacial Index	Glacial Index by Jacobsen and Dangles (2012)	-
Time since ice-free	Reconstructed amount of years, the sampling site has been free of ice	years
Q _{abs} sampling month	Modelled total glacier contribution to the discharge of the sampled stream during the month of sampling	km ³ /month
Annual CV of Q _{abs}	Annual coefficient of variation of the modelled total monthly glacier contributions to stream discharge	-
Turbidity	Streamwater turbidity	NTU
Temperature	Streamwater temperature	°C
Conductivity	Streamwater electrical conductivity	µS/cm

4 Data and Methods

4.1 Calculation of the glaciological variables related to area and length

4.1.1 Data

Table 3 Overview of the data sources for the calculation of the glaciological variables related to area and length.

Relevant field data	Digital Elevation Models (DEMs)	Aerial/satellite imagery and maps	Vector data on glaciers and catchments
GPS points of the sampling sites and snouts	High resolution DEMs (0.5 m), swissALTI ^{3D}	High resolution orthophotos (0.25m), SWISSIMAGE	'Topographical catchment areas of Swiss waterbodies 2 km ² '
Qualitative observation notes about the sampling sites and their glaciers	Medium-resolution DEMs (30 m), ASTER GDEM V3	Medium-resolution satellite images (10m) Sentinel 2, level 2a	Former glacier extents from the GLIMS database (individual source dates)
Photos of the sampling sites and glaciers		Topographic map (1:10'000) Swiss Map Raster	

To compute these glaciological variables, the following four types of data served as inputs: Fieldwork data, digital elevation models (DEMs), satellite or aerial imagery including derived maps, as well as existing vector data of glaciers and catchments (Table 3).

The relevant field data for GIS analysis include GPS points of the sampling sites and of the glacier snouts (if safely accessible), personal observation notes about the sampling sites and respective glaciers, as well as photos taken on the sampling day. The GPS points were measured with a handheld device (GPSMAP®66s, GARMIN) and have a horizontal accuracy of 15 m in 95 % of the situations (Garmin, 2021). If legally and logistically possible, the photos were complemented with images captured with a DJI Mavic 2 Zoom drone.

The extremely precise 'swissALTI^{3D}' DEM (swisstopo, 2018) served for the mapping of the Swiss glaciers, whereas for the remaining ones the elevation was derived from the globally available Terra Advanced Spaceborne Thermal Emission and Reflection Radiometer (ASTER) Global Digital Elevation Model (GDEM) Version 3 (NASA and others, 2019).

Above 2000 m, the 'swissALTI^{3D}' DEM is based on stereo-correlation of orthophotos and gets systematically updated in a 6 years interval (swisstopo, 2018). The acquisition years of the most recent DEMs available for the selected Swiss glaciers range from 2014 – 2019 and they are provided in a 0.5 m resolution with a vertical precision of 1 - 3 m above 2000 m (swisstopo, 2018).

The ASTER GDEM V3 however, is a global DEM available in a spatial resolution of 1 arc second, which corresponds to approximately 30 m (NASA and others, 2019), with a standard deviation of the elevation error of 12.1 m (Abrams and Crippen, 2019). All ASTER Level 1A scenes acquired between 2000 – 2013 were used to produce over one million individual scene-based ASTER DEMs by stereo correlation. In a second step, cloud masking was applied and they were stacked, residual bad values and outliers were removed and finally, the DEM was corrected for residual anomalies using several

existing reference DEMs (NASA and others, 2019). Given its coverage spanning from 83° North to 93° South, void free-data were available for all sampling destinations, including Greenland. The individual DEM tiles were downloaded from <https://search.earthdata.nasa.gov/search>. Raster cells with erroneous data remain possible and were addressed by drawing glacier center-line transects in GIS and double-checking the plausibility of their shapes; without any alarming observations.

In order to map the current extents of the Swiss glaciers, both the orthophotos and topographic map provided by the Swiss Geoportal (swisstopo, 2021a) were used in parallel. The layer 'SWISSIMAGE' is a composition of digital orthophotos with 25 cm ground resolution and a horizontal precision of 25 cm in the mountainous part of the country (swisstopo, 2020). It is getting updated in a 3 years cycle (swisstopo, 2020), with acquisition years ranging from 2016 – 2019 in case of the imagery used. The topographic maps derived from these images are available in a scale of 1:10'000 – 1:1 Mio and get completely updated in ca. 6 years intervals (swisstopo, 2021b).

Due to the lack of accessibility to comparable orthophotos or high-resolution maps in the case of the non-Swiss glaciers, the mapping of these latter was performed using Sentinel 2 satellite imagery, retrieved from <https://scihub.copernicus.eu/>. The chosen processing level 2a provides an orthoimage Bottom-Of-Atmosphere corrected reflectance product containing 13 spectral bands (ESA, 2021). Since not all of these bands are available in a 10 m resolution, only the True Color Image (TCI) in 10 m resolution together with the lower resolution Water Vapor map and Scene Classification map products were used for glacier mapping. Despite the temporal resolution of 10 days, it was not trivial but still essential to find scenes with minimal seasonal snow, as well as little or no shadow and cloud cover above the areas of interest. For this purpose, a pre-filter for cloud cover of less than 10 % was applied and the Water Vapor and Scene Classification maps contributed to quickly evaluating the utility of a scene. Regarding the snow cover, only scenes with sensing dates during the respective ablation season were chosen and the scenes that had passed this filter were thoroughly compared with others and analyzed using the Scene Classification map in order to detect some potential seasonal snow.

The fourth mentioned category of data are the vector ones or in other words polygons representing either catchments or former glacier extents. The vector dataset 'Topographical catchment areas of Swiss waterbodies 2 km²' accessed on the Swiss Geoportal facilitated the catchment classification in the case of the Swiss glaciers. Former glacier outlines derived from the Global Land Ice Measurements from Space (GLIMS) database (Raup and others, 2007) were used as templates to adjust these polygons to the current glacier extents. The availability of recent glacier outlines on this global inventory and their quality greatly depends on how frequently and accurately local glacier inventories are produced and revised, but unfortunately for several of the sampling destinations no glacier outlines from the last decade were yet available.

4.1.2 GIS Analysis

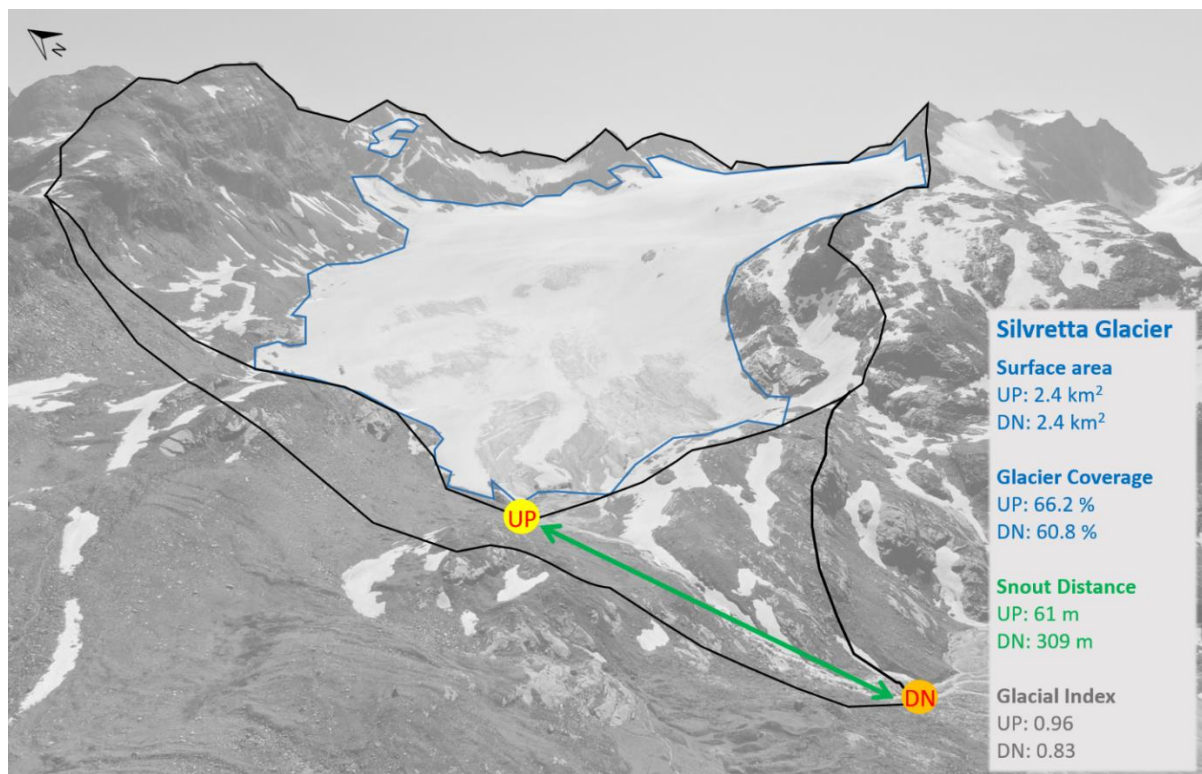


Figure 4 Remotely sensed glaciological regression variables at the example of Silvretta glacier (CH). The catchments above the UP- and DN-sites are illustrated in black and the glacier surface area in blue. The photo was taken on the sampling day (July 10 2020) and shows some remaining seasonal snow.

In order to explain the steps involved in the calculation of the glaciological variables, first the underlying glacier definition needs to be clarified. In the case of this study, it differs from the definition used by the GLIMS initiative:

“A glacier or perennial snow mass, identified by a single GLIMS glacier ID, consists of a body of ice and snow that is observed at the end of the melt season, or, in the case of tropical glaciers, after transient snow melts. This includes, at a minimum, all tributaries and connected feeders that contribute ice to the main glacier, plus all debris covered parts of it. Excluded is all exposed ground, including nunataks. (...)”(Raup and Khalsa, 2010).

For the Vanishing Glaciers project, a specific, more hydrological glacier definition was chosen, which better fits the needs of stream ecology research. It agrees with all the other requirements mentioned above, but defines the glacier’s surface area as the total glacierized area in the catchment above the sampling location. In other words, what is characterized as one glacier can include only part of or more than one GLIMS glacier entity. A visual example of this definition and of the derived glaciological variables is provided in Figure 4. Hence, in order to calculate the variables surface area, glacier coverage and Glacial Index, first, the glacier surface- and the catchment area need to be determined, using the GIS techniques described in the following paragraphs.

In a first step, sampled glaciers were clustered into groups located on the same hemisphere with similar longitude. This allowed to conduct the GIS analysis in the respective local WGS 1984 UTM coordinate systems: For the European Alps and Norway combined (UTM Zone 38N), Ecuador (17S), Russia (38N), New Zealand (59S) and Greenland (22N). The GPS-points of the sampling sites were first imported and their location was visually double-checked using the Sentinel 2 imagery or SWISSIMAGE.

Once the correct location had been confirmed by other members of the field team, the catchment delineation of the Swiss glaciers was performed by combining or subdividing pre-existing polygons of the dataset ‘Topographical catchment areas of Swiss waterbodies 2 km²’ (BAFU, 2021). From the sampling coordinates, lines perpendicular to the contour lines were drawn until they reached the drainage divides provided by this dataset, which is calculated based on the SwissALTI^{3D} (swisstopo, 2018). Instead of downloading all the high-resolution visual information, the catchments were manually mapped directly in the Geoportal and later exported to ArcMap (version 10.6.1).

No such dataset existed outside of Switzerland and the delineation had to be conducted manually due to unsatisfactory results of automatic catchment classification based on hydrological analysis by the method described in Bolch and others (2010). Indeed, automatic catchment classification based on ASTER GDEM V3 seems to work well if the sampling points are locations far downstream in a valley with distinct surrounding topography. Many of our sampling points are, however, located in hummocky proglacial areas next to glaciers with similarly chaotic small-scale surface topography. As a consequence, even if the pouring point was manually moved on top of one of the raster cells classified as streambed by the ArcGIS ‘Flow accumulation’ function, this GIS workflow did not succeed in automatically detecting the catchment area of the whole glacier surface. This can be explained by the fact that the GIS algorithms only describe the flow accumulation taking place on the surface of the glacier and of the surrounding terrain, but they don’t take into account ice flow.

Hence, for the resulting manual delineation all necessary tiles of the ASTER DEM were mosaiced together and classified by applying a maximal color gradient between snout- and maximum glacier elevation, as a visual help to read the terrain. In addition, contour lines with an interval of 10 m and 20 m were generated. Based on these two sources of information plus the drainage divides which separate the GLIMS glacier entities in the accumulation zones, the catchments above the sampling point were manually delineated.

As a next task, the glacierized area had to be mapped, to allow a subsequent digital intersection with the delineated catchments. Despite the wide range of existing automated or semi-automated approaches using spectral data (as described in Paul and others, 2015), manual classification proved to be the most suitable technique to map the surface area of such few glaciers in high quality. According to Raup and others (2007), human interpretation remains the best tool for extracting glacier boundaries of high quality and accuracy given some local knowledge. This requirement was met thanks to the personal fieldwork performed in almost all of these locations, some notes about the conditions encountered, plus the drone imagery and other photos taken.

The Swiss glacier mapping was performed based on both orthophotos and topographic maps provided by swisstopo (for product details refer to sub-chapter 4.1.1), whereas for the other glaciers Sentinel 2 imagery was employed. On the one hand, available high resolution images facilitate the visual distinction between seasonal snow and ice, recognizing rock outcrops as well as identifying debris-covered areas as part of the glacier and provide a more detailed and recent representation of reality. On the other hand, maps illustrate features already interpreted by an experienced analyst. Notably for glaciers lacking such high-resolution data, the DEM and derived hillshade were used to locate the glacier boundaries based on the terrain, as suggested by Quincey and others (2014).

The project-specific definition of a glacier has already been presented at the beginning of this sub-chapter, but to take practical decisions during the process of mapping, some specifications to this

definition were added based on the recommendations by Raup and Khalsa (2010). For instance, stagnant ice masses and debris-covered parts of the glacier were included into the glacierized area. Seasonal snow fields and any rock walls that avalanche onto a glacier but don't retain snow themselves, on the other hand, were excluded.

For glaciers that had not retreated a lot since the point in time of the most recent GLIMS outline, these GLIMS polygons were used and modified instead of mapping them from scratch. Following the recommendation of Paul and others (2009), only glacier polygons greater than 0.01 km² were taken into account. Since it is not always trivial to find recent satellite scenes with optimal shadow, snow and cloud conditions in some cases multiple scenes were used for mapping. Even though more details on the uncertainties related to this mapping approach are described in the following sub-chapter, it should be stated already that two shapefiles were created per UP- and DN-catchment, one representing the maximum and one the minimum possible glacier area, to reduce interpretation uncertainty.

In order to calculate the surface area, both of these shapefiles were intersected with the one representing the catchments. Using the 'Zonal statistics' ArcMap function, the total glacierized area within the catchment was calculated for both shapefiles resulting from this overlay and the mean of the derived maximal and minimal surface area served as the final result (Figure 5). Using this absolute glacier surface value, the glacier coverage was calculated as the percentage of glacierized area within the catchment and the Glacial index was computed based on the formula presented in sub-chapter 1.1.

The computation of the distances between the glacier snout and the sampling sites was the last remaining task of this GIS workflow. When taking GPS coordinates of the snout position was not safely possible, these snout locations were mapped based on the most recent orthophotos and satellite imagery. Starting from this point, the distances were measured as straight lines. In the case of the DN sites, however, they were calculated as the sum of the straight-line distance from the snout to the UP-site plus the one from UP-site to DN-site, in order to better represent the stream path.



Figure 5 UP- and DN-catchments and maximal vs. minimal glacier surface area polygons at the example of Silvretta Glacier, CH. Map and orthophotos were used as complimentary sources of information about the catchment's current glacierization (modified from swisstopo, 2021a).

4 Data and Methods

4.1.3 Uncertainty assessment

Knowing the accuracy of the glacier outlines is crucial to be able to accurately interpret the resulting regression variables and the final result. According to DeBeer and Sharp (2007) this accuracy depends typically on three aspects:

- the resolution of the images and DEMs used for the delineation of the outlines;
- the conditions during data acquisition (i.e. seasonal snow, shadow);
- the contrast between the glacier and its surroundings (i.e. debris cover).

The last two aspects can be positively influenced by an ideal choice of satellite images, whereas the image and digital elevation model (DEM) resolution will imperatively be lower, if the analysis is conducted not just for glaciers with optimal data availability, but on a global scale. Consequently, it is essential to compare the uncertainty of glacier outlines produced based on medium-resolution satellite imagery and medium-resolution DEMs with to the ones based on high-resolution orthophotos and DEMs.

For this purpose, four small glacier inventories were produced, based on the following possible combinations of input data:

- A) Satellite images and high-resolution DEMs;
- B) Orthophotos and high-resolution DEMs;
- C) Orthophotos and medium-resolution DEMs;
- D) Satellite images and medium-resolution DEMs.

By comparing these four inventories, the sensitivity of the glacier area variables to the image resolution, to the DEM resolution and to the combined impact of the DEM and image resolution were tested. This experiment was performed for three Swiss glaciers, taking advantage of the good data availability and quality in order to quantify the differences of the outcome in relation to the choice of the input data.

An additional aim was to assess the uncertainty of the manually mapped glacier outlines of the complete sample of glaciers. This was undertaken using a method suggested by (Basnett and others, 2013) that quantifies mapping and interpretation uncertainty separately and derives a total uncertainty of the glacier outlines from the combination of these terms. Hereby, the mapping uncertainty is estimated as:

$$\text{Mapping uncertainty } (a) = N \times \frac{A}{2} \quad (1)$$

where N is the number of pixels along the glacier boundary and A is the area of the pixel.

In order to estimate the interpretation uncertainty, mainly linked to debris-covered glacier snouts or to the lack of image contrast due to shadow, alternative glacier boundaries were mapped with the aim of defining two extreme positions of the glacier extent. Hereby the interpretation uncertainty is calculated as:

$$\text{Interpretation uncertainty } (b) = SA_{max} - SA_{min} \quad (2)$$

where SA_{max} is the maximum possible glacier extent and SA_{min} is the minimum glacier extent. From these two uncertainty terms the total uncertainty was computed:

$$\text{Total uncertainty} = \sqrt{a^2 + b^2} \quad (3)$$

Based on the results of these two uncertainty assessments, the glacier surface area and glacier coverage of the catchment can be complemented with corresponding error bars.

For the snout distances, no particular uncertainty assessment was performed. However, given the GPS accuracy of ca. 15 m (Garmin, 2021) and in case of the remotely-sensed glacier snout locations, an image resolution of 10 m or higher, the resulting distances should be assigned with an error bar of ± 30 m.

4.2 Deglaciation analysis

4.2.1 Additional data

Table 4 Supplementary data sources used for deglaciation analysis.

Swiss imagery and maps	Inventory data
Historical orthophotos 'SWISSIMAGE Journey through time', available 1979 onwards	WGMS Fluctuations of Glaciers Database – Front variation measurements
Historical maps 'Journey through time', dating back to 1844	

In addition to the GPS-points, Sentinel 2 imagery and GLIMS glacier outlines described in sub-chapter 4.1.1, Table 4 lists all supplementary data used for this task. In the case of the Swiss glaciers, historic maps served as a key source of information. Using the 'Journey through time' tool on the Swiss geoportal, the individual tiles of the Dufour map produced 1844 - 1865 in a scale of 1:100'000 (swisstopo, 2021c) and the Siegfried map dating back to 1870 - 1926 in a scale of 1:50'000 in mountain terrain (swisstopo, 2021d) can be accessed. From 1968 onwards, 1:25'000 maps started to be updated systematically in a 6 year- interval (swisstopo, 2021e), providing extraordinary high temporal resolution information about former glacier extents. The accuracy of these map products ranges from an average position error of 153 m for the Dufour map (swisstopo, 2021c), less than 75 m in case of the Siegfried map (swisstopo, 2021d) to 2.5 – 7.5 m for the maps produced 1968 onwards (swisstopo, 2021f). The same tool also exists for historic orthophoto-mosaics, which are available every ca. 6 years from 1979 onwards with a ground resolution of 0.5 m or less and a position error of maximal 3 - 5 m (swisstopo, 2021f).

To map historic glacier extents of the non-Swiss glaciers, Sentinel 2 imagery ranging back to the first acquisition year 2015 (NASA, 2021) was used. As a supplement, ASTER satellite imagery could have reached further back in time due to the mission start in 1999 (Abrams and others, 2002). However, scenes older than 2-3 years cannot be retrieved directly but need to be pre-ordered. Due to the individual length change behavior of each glacier, it remained unclear which scenes are the ones with a time stamp of interest and would need to be ordered. Hence, for glaciers with few known glacier extents, alternative reconstruction methods proved to be more efficient. One of those methods described in the next sub-chapter, takes into account annual front variation measurements provided by the Fluctuation of Glaciers database (WGMS, 2019). These observation data are available for all the non-Swiss and 12 out of 14 Swiss glaciers, but the length of the measurement records vary from few decades to more than 1.5 centuries and most of them contain data gaps.

4.2.2 Reconstruction of the time of deglaciation

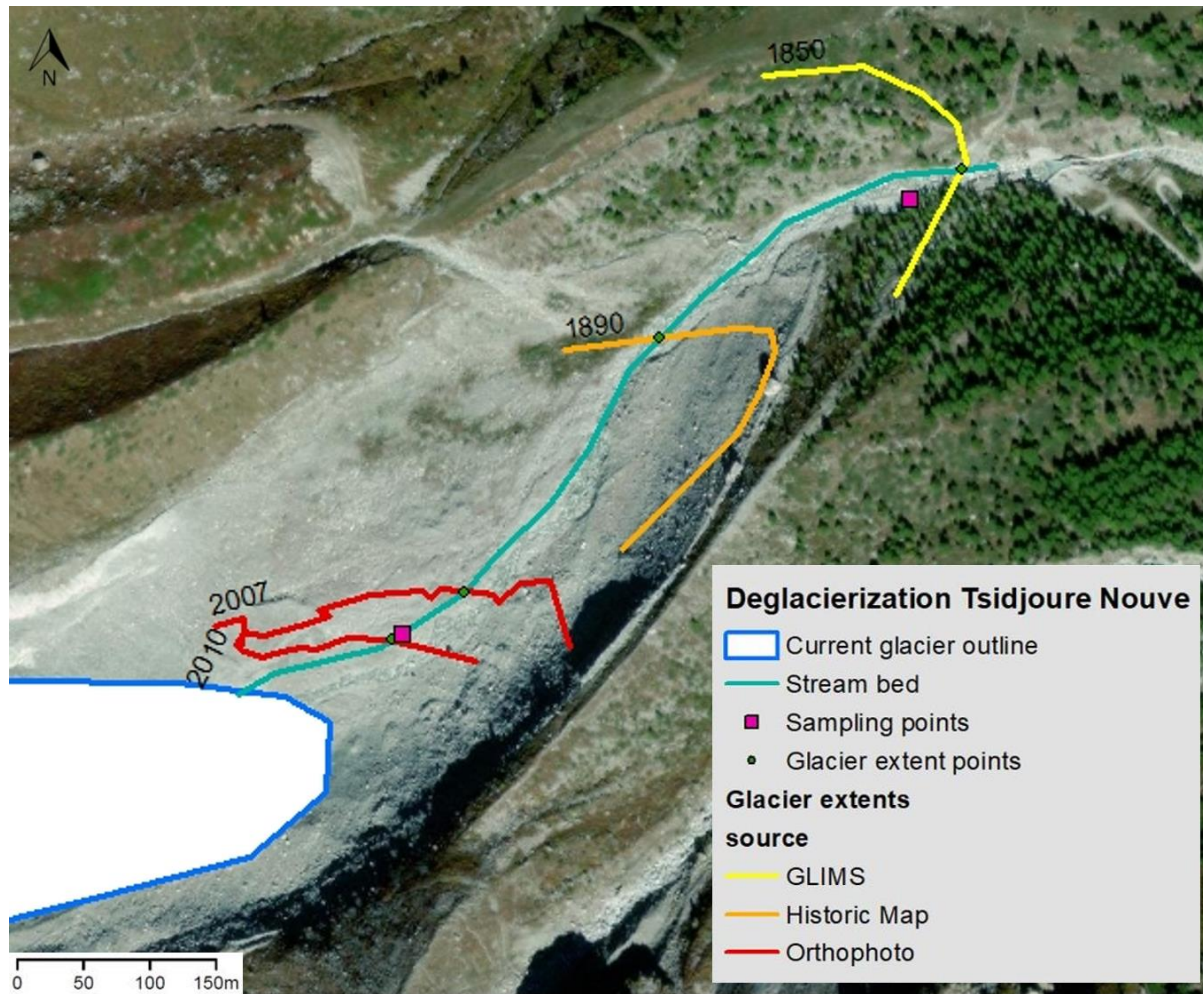


Figure 6 Known glacier extents of the Tsidjoure Nouve Glacier, Switzerland, based on different data sources. The year when the UP-site became ice-free was reconstructed using linear interpolation (method A) between the extents of 2007 and 2010. In order to reconstruct the time of deglaciation of the DN-site, absolute values of front variation (method C) were used to approximate the behavior of the glacier after 1890, since until 1895 it was still advancing remarkably. The resulting estimated years of deglaciation are 2009 in the case of the UP-site and 1898 for the DN-site (modified from swisstopo, 2021a).

To prepare this reconstruction workflow, the current stream bed was delineated based on orthophotos and maps or satellite imagery, assuming that the former flow path of the glacier corresponds to the one of the current stream. In a next step, all the known glacier extents were mapped and labeled with the corresponding years. Historic maps and orthophotos served as information sources for the Swiss glaciers, whereas Sentinel 2 imagery and GLIMS glacier outlines provided information on all the glaciers (Figure 6).

By intersecting the snout outlines with the mapped stream bed, glacier extent points were created. The extent year attribute of those points allowed to connect them to one line of consecutive year points per glacier and thereby quickly detect potential glacier re-advances, indicated by a zig-zag shaped line. Such points were marked in order to highlight this crucial information. For all the 40 sampling points, the two neighboring glacier extent points had to be identified, since the remaining workflow was determined by the time span between these two extent points. Based on the decision tree illustrated in Figure 7, for each sampling point, the most suitable of the following three methods was applied:

A) In the best case scenario, a Swiss sampling points lies in between two former glacier extents known from historical Swiss maps with a 6 years mapping interval. Across a time span of such few years, linear interpolation can easily be justified and was performed in ArcMap using the 'Create routes' function.

B) If the sampling point is located in between two extent points which cover a time span of more than 6 years but front variation data is available, the reconstruction approach was based on these observation data. The observed length variation in between these two points in time including potential re-advances was scaled to the length of the flowline segment between these two extent points. In case of data gaps, the mean annual length change value over the timespan without data were assumed as annual length change values.

C) If front variation measurements are available but a sampling point is located further downstream than the oldest known glacier extent, scaling as described in method B was not possible. Instead, the reconstruction was performed starting from the single known neighboring glacier extent point using the absolute length change values. As described in method B, data gaps were filled with mean annual length change values averaged over the time span of the data gap.

Method C) had to be applied for the DN-sites of five glaciers, namely Antizana α , Chamberlin, Djankuat, Storbreen and Tsidjoure Nouvelle. In the case of Hohlaub-N Glacier, the DN-site is located between two extent points referring to extents that lie 39 years apart. Since no front variation data are available for the time span of interest, the reconstruction had to be performed using method A). The results of all three methods were expressed as years of deglaciation and will be presented in sub-chapter 5.2.2.

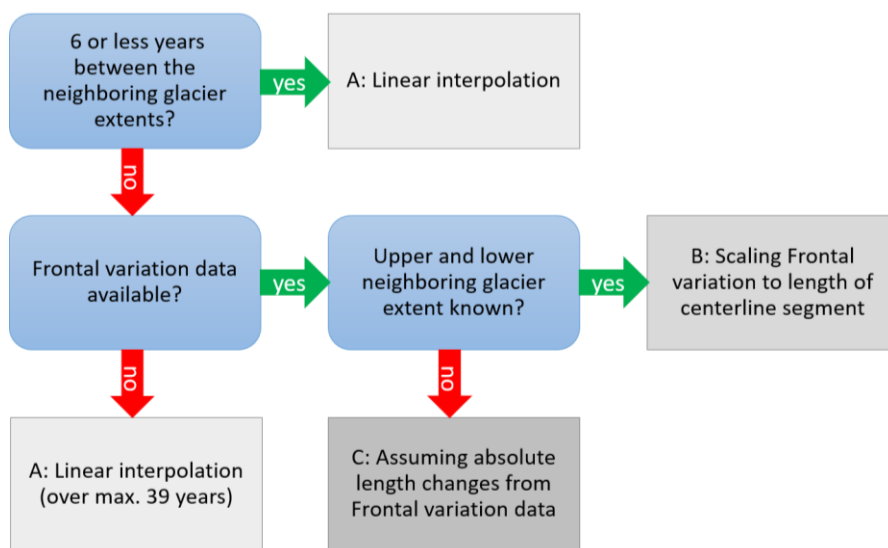


Figure 7 Decision tree for the deglaciation analysis. Depending on the available data sources the reconstruction was performed using method A, B, or C.

4 Data and Methods

4.3 Discharge estimations

4.3.1 Modelling data

The discharge estimates were based on the results of existing hindcast model runs of the Global Glacier Evolution Model (GloGEM). This process-based model calculates mass balance and associated geometric changes in response to climatic forcing for each of the roughly 200'000 glaciers of the planet (Huss and Hock, 2015). The model structure, as well as its input data (downscaled monthly air temperatures provided by 14 general circulation models from the Climate Intercomparison project CMIP5 (Taylor and others, 2012)) are described in detail in Huss and Hock (2015). The same holds true for the process of calibration using observed glacier mass changes (Gardner and others, 2013) and the model validation based on in situ measured data from the World Glacier Monitoring Service (WGMS, 2012). The model was developed to estimate future global glacier mass changes and sea-level rise (Huss and Hock, 2015, 2018). However, for the purpose of this study, 37 years of hindcasting model runs (1980 – 2016) provided by the authors, were used to estimate the mass balance of the 20 individual glaciers.

4.3.2 Calculation of the discharge variables

Once the modelled specific monthly discharges for each glacier were uploaded into RStudio, the file had to be transformed into a format that allows the comparison and analysis of these time series. This step included i.e. the creation of one table row per observation and assuring that the dates of the hydrological year between the northern and the southern hemispheres were interpreted correctly. The modelling outputs estimate the glacier mass changes of every individual glacier polygon of the Randolph Glacier Inventory (RGI, Pfeffer and others, 2014). Hence, in a next step, for each of the 20 glaciers considered in this study, the respective RGI-IDs had to be identified. Owing to the project-specific glacier definition (sub-chapter 4.1.2), in many cases one sampled glacier corresponded to multiple RGI-IDs and thus, a polygon overlay was performed to attribute all the necessary RGI-polygons to each of the 20 glaciers. Next, the polygon's surface areas were recalculated based on my personal, more recent mappings that were labeled with the corresponding Vanishing Glaciers project glacier IDs. The modelling results were formulated as specific monthly discharges in meters water equivalent (m.w.e.) per RGI-ID. By multiplying these values with the individual surface areas per polygon and summing up those absolute discharges for each Vanishing Glaciers ID, the total absolute discharge values in m³/month were calculated. Based on the resulting new dataset, two regression variables were computed.

The first variable, the Q_{abs} sampling month, is an estimate of the total glacier contribution to the discharge of the stream during the specific sampling month. To calculate it, the dataset of absolute monthly discharges was filtered by the respective sampling months. In a second step, the variable was calculated as the mean value of Q_{abs} sampling month of the last five hydrological years (2012 - 2016). The first reason to average it across this timespan was the fact that many of the sampling sites have become ice-free very recently (sub-chapter 5.2.2). Secondly, from the visual inspection of the hydrographs of the last 37 years (Appendix 6), it became apparent, that the monthly discharges of many streams had increased significantly in these last five years, compared to the 32 years before.

As a second variable, the annual coefficient of variation (CV, the standard deviation divided by the mean) of the modelled total monthly glacier contributions to stream discharge was computed. It serves as a measure of the flashiness of the discharge in the course of the year. First, the dataset of

the absolute discharges was subset for the ablation months with discharges of $Q_{\text{abs}} > 0$. Across these values, the CV was calculated for each year by dividing the standard deviation by the mean value. In order to be consistent with the approach used for Q_{abs} sampling month, the resulting annual CVs were also averaged across the last 5 years of the dataset.

4.4 Fieldwork

The samples and measurement data for this thesis were collected in the course of the first 7 Vanishing Glaciers project field campaigns, between January 2019 and September 2020 (for exact sampling dates refer to

Appendix 9). Very thorough planning plus large amounts of flexibility were needed to accommodate all these expeditions in the respective glacier melt seasons and deal with the administrative and logistical challenges associated with accessing these regions and glacier snouts, as well as guaranteeing a constant cooling chain at $-80\text{ }^{\circ}\text{C}$ for the samples. As mentioned in the selection criteria in sub-chapter 3.1, several scientific and practical requirements had to be met to be able to sample a specific glacier-fed stream. Hence, before making the final selection, the glacier and stream characteristics and current conditions had to be investigated very carefully using GLIMS and WGMS glacier inventory data (Raup and others, 2007; WGMS, 2019), maps, Google Earth and by inquiring local knowledge. Nevertheless, our team of four still experienced many factors hard to control (i.e. availability of running water due to latest weather conditions). The following two sections describe the two fieldwork tasks relevant for this thesis, which were performed twice per sampling day, once at the upper and once at the lower sampling site (sub-chapter 3.2). Uncertainties related to these measurements will be discussed in sub-chapter 0.

4.4.1 Sediment sampling and analysis of chlorophyll a

The sediment for chlorophyll a analysis was taken from three individual patches within a 5 m radius using flame-sterilized scoops. To acquire the desired grain size range of $250\text{ }\mu\text{m} - 3.15\text{ mm}$, these top 5 cm of streambed sediment were passed through graded sieves (Photos 2). The sediment was then transferred into sterile cryovials (10 g of wet sediment) and immediately flash-frozen in either liquid nitrogen or dry ice. After transport to the lab and storage at $-80\text{ }^{\circ}\text{C}$, chlorophyll a analysis was conducted. For each of the three replicates representing the three patches from each stream sampling location, three technical measurements were performed following the protocol described in Kohler and others (2020) and reported as $\mu\text{g Chl a g}^{-1}\text{ DM}$ (dry mass). This results in a total amount of 360 measurements (20 glaciers x 2 sites x 3 replicates x 3 measurements).

4.4.2 Measurements of physicochemical stream variables

From all the *in-situ* measured streamwater properties (see sub-chapter 3.3), turbidity, electrical conductivity and temperature were selected as the relevant ones to explain biofilm biomass variations. Streamwater turbidity was measured in a glass vial freshly filled with stream water, that was inserted into a calibrated portable turbidity meter (Turb® 430 IR, WTW). The resulting values of three consecutive measurements were reported in nephelometric turbidity units (NTU). Electrical conductivity and temperature however, were measured directly in the stream (Photo 2D) using a multi-parameter probe (MultiLine® Multi 3630 IDS, WTW, Germany). To conduct this single measurement,

4 Data and Methods



Photos 2 Sediment sampling and measurement of physicochemical stream variables. The sediments had to be A) sieved, B) transferred into cryovials and C) flash-frozen and transported at -80 °C. D) In the meantime, probes were immersed into the stream to measure temperature and conductivity (Photos: Matteo Tolosano (A and C) , Jamani Caillet (B and C)).

it was essential to perform a proper calibration and to keep the probe in the water, until the displayed measurement values had stabilized.

4.5 Statistical analysis

The following sub-chapters will address the steps and decisions involved in statistical analysis, which was performed in RStudio.

4.5.1 Detection and handling of outliers

Outlier detection can be critically important in regression analysis – because extreme values resulting from erroneous measurements or sample contamination can have large leverage on model slopes (Zuur and others, 2010). However, given the relatively small size of the dataset ($n = 40$), outlier removal had to be restricted to only a few data points. Despite other ways to identify potential outliers based on statistical distribution of points (e.g. values 1.5 interquartile ranges smaller or larger than the quantiles can be considered outliers), I opted for a combination of statistical distribution (see above) and likelihood for erroneous measurement or samples' contamination. Based on this, I removed one observation with an extreme value of turbidity and one with the same for chlorophyll a.

In terms of turbidity, this suspicious data point was an observation at the Arolla Bas DN-site. Its turbidity value of 1048 NTU was measured 1.2 km downstream of the upper site, where the day before, we had observed 91 NTU. The DN-site measurement marks the upper limit of the range of values which can be detected by the turbidity meter. In this case it was clearly the consequence of a large rainfall event (the sampling of the DN-site had to be postponed to the next day), resulting in extraordinarily turbid water. Consequently, this observation was excluded from the analysis as recommended by Zuur and others (2010) for such unusual events.

Visual inspection of the chlorophyll a measurements (Appendix 10 and Figure 16) showed one very high mean value (more than 3x larger than the highest remaining mean values) of the nine measurements at the lower sampling site of the Forno Glacier (CH). As clearly visible on Photo 3, stream banks of this sampling site were densely vegetated. I suspect that contamination of our samples by adjacent vegetation could contribute to this extreme value of chlorophyll a. However, since there is no way to reassure this, regression analyses were conducted both by including and excluding this extreme value. Multiple runs of simple and multivariate linear regression showed that calculations based on data sets either including or excluding this extreme value of chlorophyll a led to very similar results.



Photo 3 Heavily vegetated stream banks at the DN-site of Forno Glacier (CH). In this case a contamination of chlorophyll a from outside of the stream cannot be precluded.

4 Data and Methods

4.5.2 Model choice and assessment of the dataset's statistical power

I opted for a linear multivariate regression model to assess the statistical significance of various glaciological and *in situ* measured variables in explaining chlorophyll a concentrations. The strength of multivariate linear regression lies in its ability to simultaneously consider several important variables – which is often the case in ecological datasets. For instance, algal growth (measured by chlorophyll a concentration) might simultaneously depend on streamwater temperature, light and nutrient availability and streambed stability. Any of these factors could independently from the others have a strong impact on the ability of algae to grow in glacier-fed streams. However, to avoid arbitrary comparisons I first formulated a number of ecological hypotheses for the various variables. These hypotheses serve as a backbone to guide the multiple regression modelling. Additionally, I also assessed the individual influence of these variables by means of simple regression analysis and checked whether the general trend of the influence (i.e. positive or negative influence) on chlorophyll a corresponded to the respective hypothesis. The actions taken to avoid collinearity of the variables and the testing of other model assumptions will be described in the next sub-chapter.

Regarding the statistical power of this study's dataset, I consider the glaciological and physicochemical stream variables that were obtained from 20 glaciers around the world. For each glacier, we retrieved samples from an UP- and a DN-site, and at each site, samples from three patches were taken. For the determination of chlorophyll a, three technical replicates were analyzed, resulting in a total of $20 \times 2 \times 3 \times 3 = 360$ measurements of chlorophyll a. Given the remoteness and the large geographical spread among samples, this represents a significant sample size. However, glacier-fed streams are influenced by a multitude of variables that result from local and regional factors. Besides the glaciological variables that I obtained for these sites, I included potentially important physicochemical streamwater variables (turbidity, stream water temperature and conductivity). From the GloGEM model outputs I further extracted the total absolute discharge during the sampling month and the seasonal variation of discharge. Because the individual impact of each of these variables on chlorophyll a concentrations is not known and the potential interactions among these variables remain unclear, it is not possible to assess the statistical power of the entire dataset. However, observing strong ecological patterns across geographically distant sites often requires massive datasets and hence, the analyzed dataset might be too small to reveal clear patterns. Nevertheless, even non-significant trends represent an important contribution to understand the factors that potentially influence the ability of algae to grow in glacier-fed streams.

4.5.3 Testing the model assumptions

Testing the model assumptions for multivariate regression based on the recommendations described in <https://www.methodenberatung.uzh.ch> led to the conclusion that actions had to be taken regarding the normal distribution of the data and to avoid multicollinearity among the regression variables.

The distributions of all variables were first assessed using histograms and by the Shapiro-Wilk test to assess their potential deviations from the log-normal distributions (Ernste, 2011). Based on the test results that showed deviations from log-normality of the dataset, the variables were then log-transformed to approach the normal distributions. As suggested by Kohler and others, (2020) a constant of $0.65 \times$ the variable value of the smallest non-zero datum was applied to each analyte if necessary, to allow log-transformation of zeros that may result from variable values below the limit of detection.

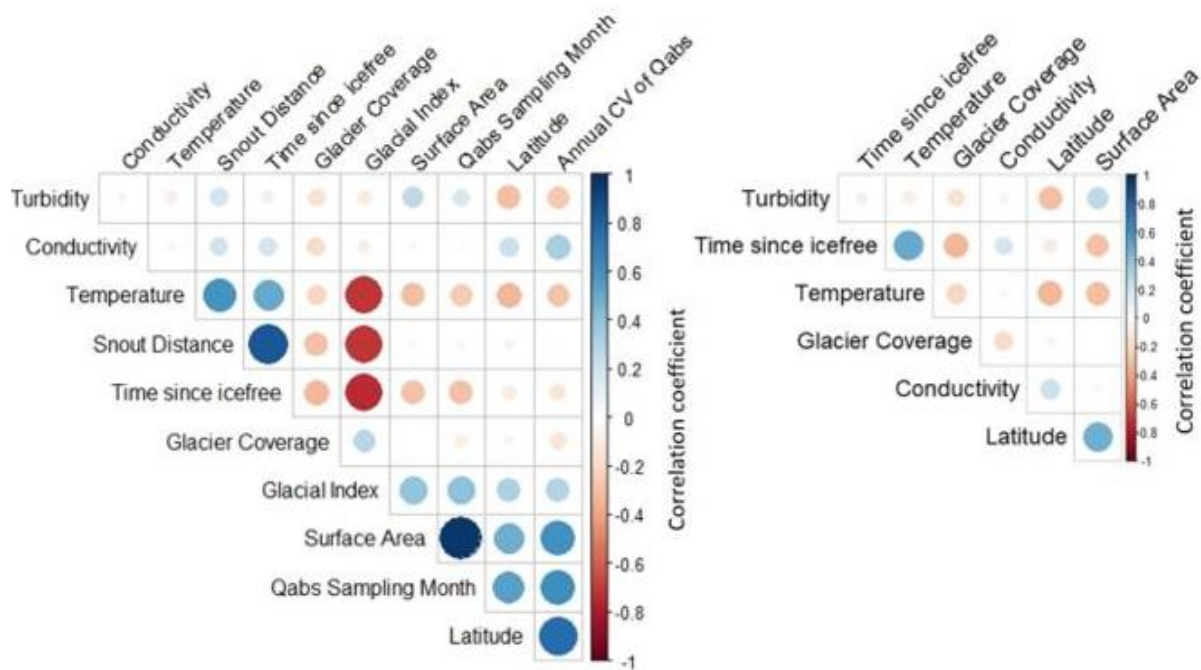


Figure 8 Multicollinearity before and after removing regression variables based on their variance inflation factors. The small correlogram represents one of many variable combinations which have been used as inputs for subset selection. Color intensity and size of the circles are proportional to the correlation coefficients.

As it can be assumed based on the ecological hypotheses described in sub-chapter 5.1, many of the selected variables are suspected to be strongly collinear. Multicollinearity is present when two or more of the predictors in a regression model are moderately or highly correlated with one another (Ernste, 2011). An approach to reduce multicollinearity is to calculate variance inflation factors (VIFs). These are measures of how much the variance of each independent variable is influenced by its correlation with the other independent variables (Ernste, 2011). The VIFs were calculated in *R* and in a next step, the variable with the highest VIF value was sequentially dropped and the VIFs recalculated, until they all reached a value <3 . This represents a more stringent approach, whereas some authors also accept VIFs <10 (reviewed in Zuur and others, 2010). This process was repeated several times (also by experimenting with removing the second-highest value, etc.) in order to create many different sets of variables with an acceptably low level of multicollinearity, that could be later used as the inputs for the best subset selection (sub-chapter 4.5.4). An example of a set of variables before and after the described procedure is illustrated in Figure 8. In this specific case the variables snout distance, Glacial Index, surface area and Q_{abs} of the sampling month had to be removed due to their moderate or strong correlations with one or more of the remaining variables.

4 Data and Methods

4.5.4 Variable selection

In order to avoid risking to miss out on a performant model, variable selection was conducted using best subset selection. This automated approach tests all possible combinations of the predictor variables and then selects the best model based on some statistical criteria (Kassambara, 2021). The necessary R-code was accessed on <http://www.sthda.com>. In a first step, the desired maximum of variables to incorporate into the model had to be specified. As shown in the example in Figure 9, this corresponded to the number of remaining variables (in this case seven) after the described procedure of removing variables with high variance inflation factors. As a response, the function returned the best single- to 7-variables models.

1 subsets of each size up to 7 Selection Algorithm: exhaustive							
	Latitude	Surface_Area	Glacier_Coverage	Time_icefree	Temperature	Conductivity	Turbidity
1	**	**	**	**	**	**	**
2	**	**	**	**	**	**	**
3	**	**	**	**	**	**	**
4	**	**	**	**	**	**	**
5	**	**	**	**	**	**	**
6	**	**	**	**	**	**	**
7	**	**	**	**	**	**	**

Figure 9 Suggested seven models containing the seven remaining variables after the procedure of strictly removing the variable with the highest VIF, until no variables with $VIF > 3$ were left

In a second step, and once the selection of statistically robust models lacking collinearity had been performed, another R-function was used to rank the suggested models based on statistical performance metrics. The application of this function yields combinations of variables with maximum adjusted R^2 , low Mallows' Cp and low Bayesian information criterion (Figure 10, Kassambara, 2021).

	Adj. R2	CP	BIC
1	4	3	3

Figure 10 Assessment of the best models according to three model performance metrics.

However, in the case of my input data, testing whether the suggested models, as well as each of their components are significant ($p < 0.01$), proved in most cases more important than this ranking. This task was performed by calculating the summary statistics of the suggested model (Figure 11). In the case of the 4-variable model, not all components were significant, whereas the 3-variable model (later referred to as 'model 1') was accepted as a potential model. Since model 3 was also recommended

```
Call:
lm(formula = chlorophyll_a ~ turbidity + temperature + surface_area +
    glacier_coverage)

Residuals:
    Min       1Q   Median       3Q      Max
-2.2968 -0.7432  0.2098  0.6621  1.7021

Coefficients:
            Estimate Std. Error t value Pr(>|t|)
(Intercept)   -3.6968    0.6980  -5.296 7.09e-06 ***
turbidity       -0.5979    0.1540  -3.883 0.000453 ***
temperature     0.2927    0.1692   1.730 0.092762 .
surface_area    0.4540    0.2001   2.269 0.029733 *
glacier_coverage -1.0780    0.8329  -1.294 0.204292
---
Signif. codes:  0 '***' 0.001 '**' 0.01 '*' 0.05 '.' 0.1 ' ' 1

Residual standard error: 1.065 on 34 degrees of freedom
Multiple R-squared:  0.3814, Adjusted R-squared:  0.3087
F-statistic: 5.241 on 4 and 34 DF, p-value: 0.002127
```

Figure 11 Summary statistics for the 4-variable model. According to the p-values highlighted in grey, the model is overall significant and the input variables can explain 30.8% (adj. R2 highlighted in yellow) of the variation in chlorophyll a. However, the model had to be excluded from subsequent model selection since most of the individual components were not significant.

according to two out of the three performance metrics, this was statistically confirmed to be a good choice.

These variable- and model selection procedures were repeated for all the sets of possible combinations of input variables. The process led to additional potential models (sub-chapter 5.5.2) and their performance will be discussed in sub-chapter 6.1. Besides the best subsets approach, forward variable selection was also performed, but did not result in any additional, overall significant models.

5 Results

5.1 Summary of the variables and underlying hypotheses

By combining glaciology and stream ecology through literature review and expert discussions, the following hypothesized links between glacier variables and chlorophyll *a* were established (Table 5).

Table 5 Glacier variables with their hypothesized effect on chlorophyll *a*.

Corr. direction	Variable	Underlying ecological hypotheses
—	Q _{abs} sampling month	<p>Increased absolute discharge has implications for:</p> <ul style="list-style-type: none"> - the shear stress scouring biofilms (Allan and others, 2021), - the bed load, as well as suspended sediment load leading to abrasion of biofilms (Bernhardt and others, 2018), - streamwater turbidity, which decreases light availability (Sommaruga, 2015; Battin and others, 2016). <p>However, without knowing the width of the stream, this modelled discharge can only serve as an estimate for the actual hydraulic conditions in the stream.</p>
—	Surface area	<p>At a given specific discharge, larger glacier surface area leads to higher absolute discharge (Benn and Evans, 2013). As seen for 'Q_{abs} sampling month', higher discharge is expected to have a negative impact on biofilm biomass.</p>
—	Glacier coverage	<p>The percentage of glacier cover in the catchment determines the contribution of ice melt to total discharge (Milner and others, 2009) with implications for:</p> <ul style="list-style-type: none"> - temperature (lower in streams with higher glacier coverage (Uehlinger and others, 2010)). - turbidity (higher, the more glaciated (Uehlinger and others, 2010)). - nutrient availability (glaciers liberate phosphate from bedrock, while nitrogen depends mainly on atmospheric deposition (Ren and others, 2019). Thus N/P ratios that are generally associated with phototrophic growth are expected to be higher in streams with lower glacier coverage (Elser and others, 2020). <p>The implications of glacier coverage for these physicochemical stream properties lead to the assumption of a negative correlation.</p>
—	Glacial Index	<p>Glacial Index acts as a surrogate for the effects of both surface area and snout distance on biofilm biomass and thereby serves as a proxy for environmental harshness (Jacobsen and Dangles, 2012). Since environmental harshness declines with decreasing Glacial Index, the correlation is expected to be negative.</p>
—	Latitude	<p>Through variations in solar radiation, latitude is one of several factors (i.e. aspect, shading, streamwater turbidity) controlling the light availability at the stream bed (Allan and others, 2021). During the windows of opportunity in spring and fall, less light may be available to the primary producers at high latitude as compared to lower latitudes.</p>

—	Annual CV of Q_{abs}	The coefficient of variation of the modelled monthly glacier contributions to stream discharge is a measure of the relative magnitude of discharge peaks and hence related to streambed stability. The higher its value, the flashier the hydrologic regime and the less stable are streambeds. Streambed stability is crucial for biofilm growth since disturbances can lead to mechanical damage of the biofilm (Bernhardt and others, 2018).
+	Time since ice-free	Streambed stability is a function of the time since deglaciation (Gurnell and others, 1996). As seen above, this stability is crucial for biofilm growth. While positive effects of time since ice-free are observable over long time scales, it is unclear whether more recent glacier recession would allow for sufficient stabilization of streambeds. Thus, depending on sediment supply, glacier coverage and time scale, the longer a sampling site has been free of ice, the more biomass could be expected.
+	Snout distance	Based on a space for time substitution and according to Gurnell and others (1996), streambed stability tends to be higher the farther away the sampling site is located from the glacier snout. Increasing downstream water temperatures (Uehlinger and others, 2010) additionally support the expected positive correlation.

The same information was gathered for the relevant *in-situ* measured physicochemical stream variables, as listed in Table 6.

Table 6 Physicochemical streamwater variables with their hypothesized effect on chlorophyll *a*.

Corr. direction	Variable	Underlying ecological hypotheses
—	Turbidity	Turbidity reduces light reaching the streambed and thus light available for photosynthesis (Davies-Colley and Smith, 2001). Since turbidity is caused by suspended sediment particles, this variable also integrates the effects of ‘scouring’, mechanical abrasion of biofilms due to suspended sediment (reviewed in Bernhardt and others, 2018).
+	Conductivity	This property refers to the abundance of dissolved ions and is used as a surrogate for subglacial and stream chemical weathering (Cano-Paoli and others, 2019). Conductivity also reflects the contribution of groundwater to GFS and some of these ions might be important nutrients (i.e. PO_4^{3-} , T. Kohler pers. comm.). Under the assumption that positive effects of conductivity are not overwhelmed by increased suspended particle loads, one might thus expect a positive association between stream water conductivity and chlorophyll <i>a</i> .
+	Temperature	Lower temperature generally leads to lower metabolic rates, which results in slower growth (Milner and Petts, 1994; Brown and others, 2004; Elser and others, 2020). However, some algae seem to be very well adapted to cold water temperature (Milner and others, 2009). Nevertheless, since temperature may also capture aspects of other important variables (i.e. large glacier coverage, high discharge), we hypothesize a positive correlation.

5 Results

5.2 Visualization of the individual glaciological and physicochemical variables

This sub-chapter provides a visualization of the calculated variables described in the methods sub-chapters 4.1 - 4.4, which later served as regression inputs. Additionally, the results of uncertainty analysis will be addressed.

5.2.1 Glacier area and length variables

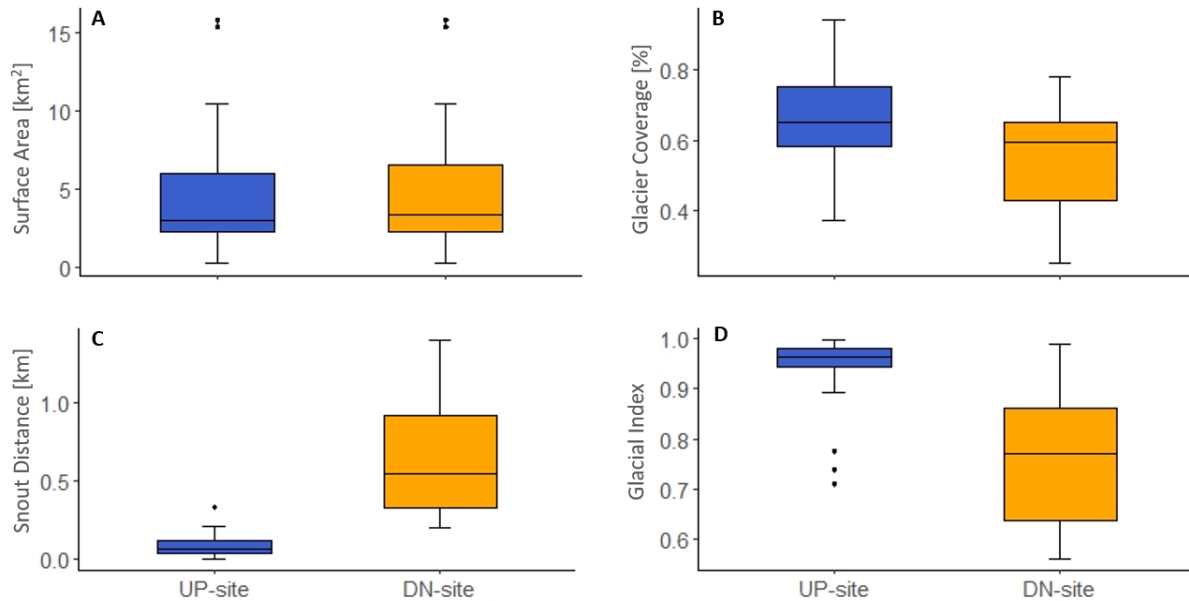


Figure 12 Visualization of the spread in observations for the regression inputs surface area, glacier coverage, snout distance and Glacial Index.

The absolute surface area of the sampled glaciers ranged from 0.29 km² (Antizana 15 α , EC) to 15.77 km² (Morteratsch, CH, Figure 12A). The surface area of Morteratsch and Findelen Glacier (CH) were significantly larger than the remaining 18 glaciers. As the results show, the surface areas of the DN-site can be larger than the UP-site of the same glacier due to the project-specific glacier definition as the total glacierized area within the catchment above the sampling site. The resulting glacier coverages spanned a range from 25% at the DN site of Valsorey (CH) to 94 % in the case of Chamberlin (GL) with the large majority of UP-sites corresponding to a glacier coverage of more than 50 % (Figure 12B). Obviously, glacier coverages were strongly linked to the distance between the glacier snout and sampling site and the resulting catchment area. These snout distances ranged from 2 m at the UP-site of Morteratsch (CH) to 1400 m (Tschierwa, CH) for the farthest DN-site (Figure 12C). The UP-sites of Hintereisferner (AT) and Hohlaub-N (CH) were sampled at greater distance to the snout than some DN-sites in our dataset; however, these streams were also sampled several 100 m downstream (DN-site).

The combined impact of absolute surface area and snout distance as a proxy for environmental harshness is reflected by the Glacial Index, with values ranging from 0.56 in the case of Antizana 15 α (EC, sampled 418 m downstream of the very small glacier) to a maximum of 0.999, 2 m from the snout of Morteratsch (CH, Figure 12D). The choice not to include sampling sites below confluences with other sources of water or after any kind of intermittency or lakes (as outlined in sub-chapter 3.2), resulted in a data set with only Glacial Indices larger than 0.5.

As described in sub-chapter 4.1.3, two types of uncertainty assessment have been performed to better understand how uncertainties affect the resulting values of surface area and other variables which include surface area. According to the method of Basnett and others (2013), mean total uncertainty of

the absolute surface area results in 3.1 %, with a lower average among the Swiss glaciers (2.9 %) than among the non-Swiss glaciers (3.7 %, Appendix 3). Along with the interpretation uncertainty term, the one about the mapping uncertainty becomes negligible. Based on the comparison of four inventories produced for three selected glaciers (sub-chapter 4.1.3), the resolution of the images used for mapping had a higher average impact on the accuracy of the outlines (3.7 %) than the resolution of the DEM (1.3 %) or the combined resolution of DEM and image resolution (2.8 %). When analyzing the combined impacts, the effects of image resolution were compensated by the ones for DEM resolution, resulting in a lower uncertainty than the one due to image resolution. The outcomes of these two uncertainty analyses are listed in detail in Appendix 1 - 3 and in the results table (Appendix 7). There, corresponding error bars for the variables surface area and glacier coverage have been calculated based on the method by Basnett and others (2013). The uncertainty of the variable snout distance has been addressed in sub-chapter 4.1.2.

5.2.2 Deglaciation of the sampling locations

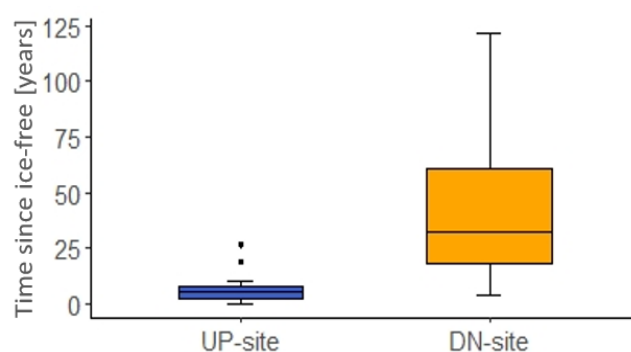


Figure 13 Distribution of the estimated amount of years the upper and lower sampling sites have been free of ice.

The reconstruction described in sub-chapter 4.2.2 resulted in estimated times since deglaciation ranging from <1 - 122 years (Figure 13). According to this estimate, all the UP-sites except for Hohlaub-N (CH) have become ice-free within the past 20 years, whereas for the majority of DN-sites this happened approximately 20 – 70 years ago.

The estimated times since-icefree are visualized in Appendix 4, whereas Appendix 5 states for each sampling site, which of the three reconstruction methods has been used including the potential uncertainty.

5.2.3 Discharge estimations

The choice and exact definition of the discharge related input variables has been outlined in sub-chapter 4.3.2. The analysis of these modelling outputs resulted in a range of absolute discharges of the sampling month (Q_{abs} Sampling Month) spanning from approximately 0.001 km³/month (Antizana 15α, EC) to 0.015 km³/month (Mortersatsch, CH, Figure 14A). Under the strongly simplified assumption that stream flow occurs at the same magnitude during the whole month (i.e. ignoring important diurnal variation), this translates into a range of 0.04 to 5.92 m³/s in the smallest and largest glacier-fed streams, respectively. The majority of monthly discharges, however, are situated in the approximate range of 0.0014 – 0.006 km³/month, theoretically equaling to 0.53 - 2.28 m³/s.

5 Results

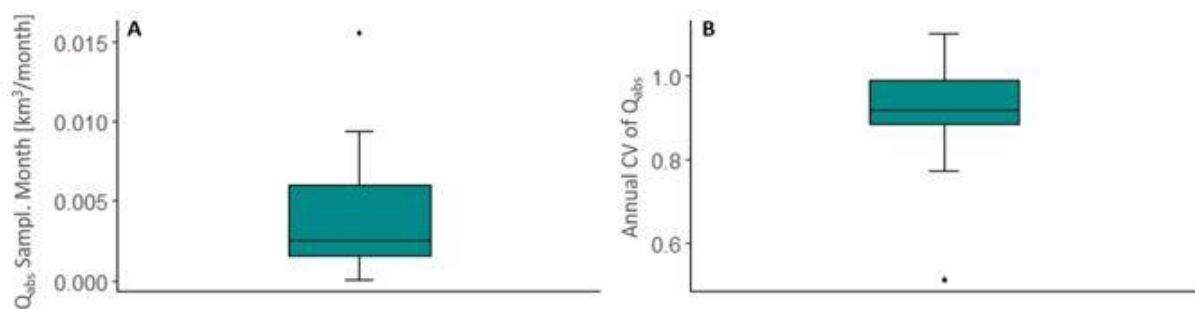


Figure 14 Distribution of A) the total absolute discharge of the sampling month and B) the annual coefficient of variation of the monthly absolute discharge.

In terms of Annual CV of Q_{abs} (the annual coefficient of variation of the absolute monthly discharges for months with discharges $> 0 \text{ m}^3/\text{month}$), a minimum coefficient of 0.51 or in other words minimal flashiness of the discharge was observed for the one glacier located very close to the equator (Antizana 15 α , EC, Figure 14B). Based on the modelling results, the maximum coefficient of 1.1 had been reached at Mont Mine (CH).

5.2.4 Physicochemical stream variables

Measured streamwater temperature ranged from 0°C at the UP-site of Tsidjoure Nouvelle (CH) to 7.9°C at the DN-site of Forno, 907 m downstream of the snout (Figure 15A). Observed temperatures were significantly higher at the DN-sites compared to the UP-sites and the underlying reasons will be discussed in sub-chapter 0.

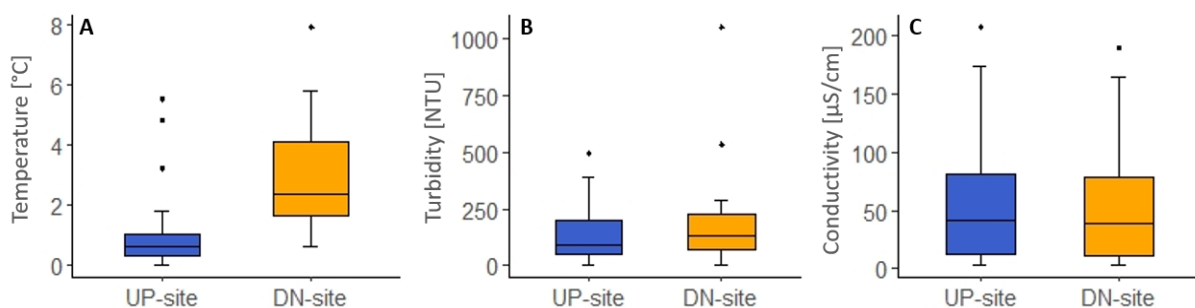


Figure 15 Distribution of measured values of A) temperature, B) turbidity and C) conductivity.

Regarding the mean value of the three turbidity measurements, a minimum of 4.53 NTU was recorded at the DN-site of Brewster (NZ, Figure 15B). After removing the outlier of 1048 NTU at the DN-site of Arolla (CH) as described in sub-chapter 4.5.1, the resulting maximal turbidity value of 533 NTU was measured at the DN-site of Antizana 15 α (EC). When comparing UP- vs. DN-sites, no clear trends in turbidity could be observed. Uncertainties regarding these measurements and the temporal variability of these properties will be addressed in sub-chapter 0.

The lowest measured electrical conductivity of $3.5 \mu\text{S}/\text{cm}$ was observed in the meltwaters of Antizana 15 α (EC), whereas conductivity reached the maximum of $207 \mu\text{S}/\text{cm}$ at Hohlaub-N (CH, Figure 15C). When comparing the two values measured per stream, hardly any variation in conductivity between UP- and DN-site could be detected. This is related to the sampling design, avoiding larger tributaries and hence pronounced changes in streamwater electrical conductivity.

5.3 Observed values of chlorophyll a

Across all sites, mean chlorophyll a concentrations were on average higher at DN sites ($0.01 \pm 0.02 \mu\text{g Chl a g}^{-1} \text{ DM}$) than at UP sites ($0.008 \pm 0.007 \mu\text{g Chl a g}^{-1} \text{ DM}$, Figure 16). No significant correlation of UP- vs. DN-site chlorophyll a values could be detected. The nine measurements of chlorophyll a per sampling site revealed a large intra-site variability. Across all sites, intra-site variability as estimated by the coefficient of variation (CV) ranged between 0.27 and 2.55 with a mean CV of 0.82 ± 0.45 . This intra-site variability was very similar at UP- (0.82 ± 0.49) and DN-sites (0.83 ± 0.4). The described extreme values observed at the DN-site of Forno Glacier are illustrated in Appendix 10.

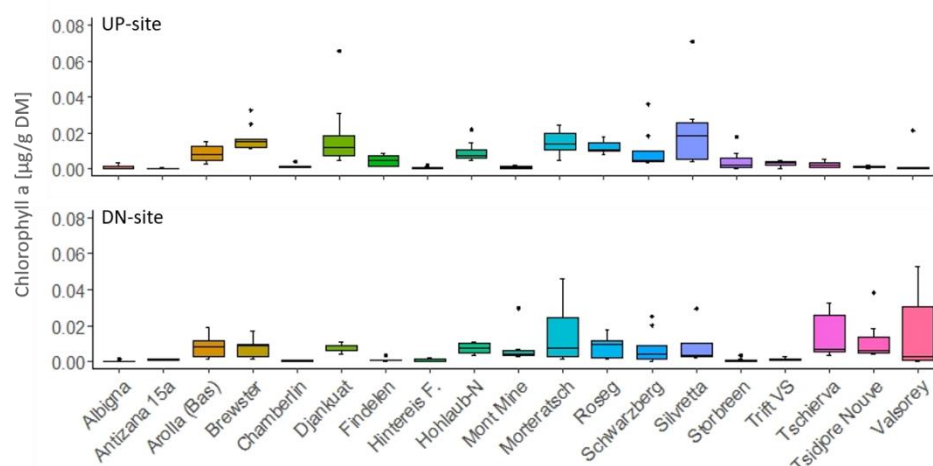


Figure 16 Inter- and intra-site distribution of observed chlorophyll a values. To ensure legibility, the extreme values measured in the stream of the Forno Glacier (CH) were excluded.

5.4 Performance of the Glacial Index in predicting chlorophyll a

Using simple linear regression, the performance of the Glacial Index in predicting chlorophyll a concentration was evaluated. The resulting coefficient of determination (R^2) of this correlation was very low and the model not significant (Figure 17). If it would have been significant, it would be stating that only 3 % of the variation in chlorophyll a concentration can be explained through the Glacial Index. The model was run with log-transformed data but the outcomes were almost identical if non-transformed values were used. Ultimately, one model run without exclusion of the extreme value in chlorophyll a (as described in sub-chapter 4.5.1) resulted in an even weaker performance of the Glacial Index. To summarize, based on this dataset no correlation between Glacial Index and chlorophyll a concentration was observed.

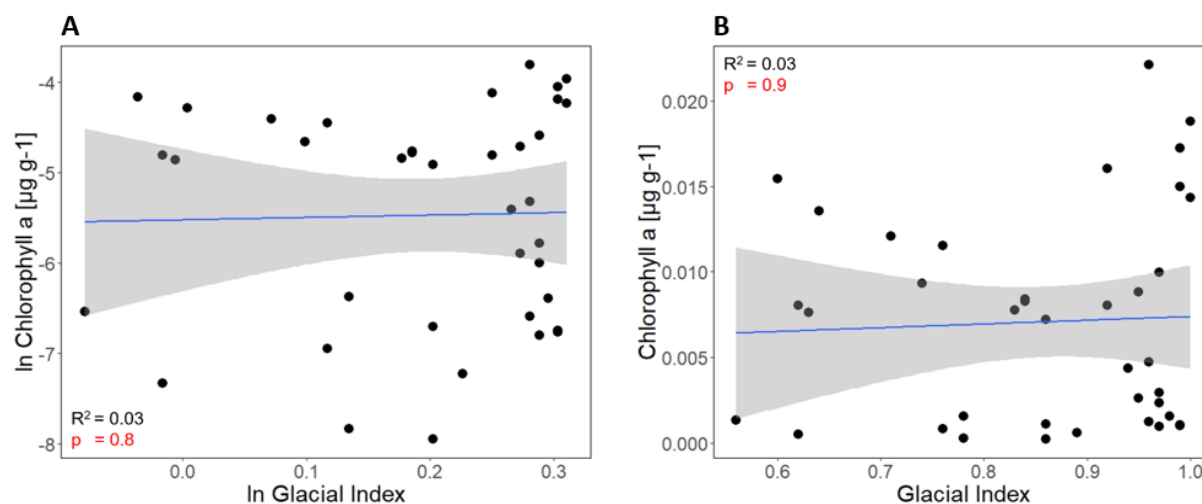


Figure 17 Performance of the Glacial Index in predicting chlorophyll a using A) log-transformed B) and raw data.

5 Results

5.5 Correlation of the model variables with chlorophyll *a*

5.5.1 Simple linear regression

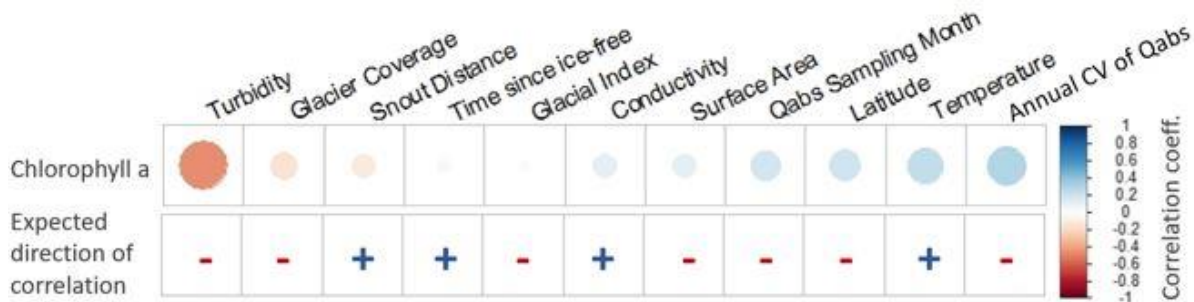


Figure 18 Performance of 11 simple linear models in predicting chlorophyll *a*, sorted by Pearson correlation coefficient. Color intensity and size of the circles are proportional to the correlation coefficients and color comparison with the second row indicates whether the modelled correlation direction corresponds to the one expected based on ecological hypotheses. The independent variables are sorted from left to right by increasing correlation coefficient.

In search of other variables which can better explain observed chlorophyll *a* concentration than Glacial Index, the performance of all selected glacier- and physicochemical stream water variables was tested in a first step using simple linear regression. The results of these additional 10 models are illustrated in Figure 18, together with the hypothesized direction of the correlation. A strongest negative correlation between chlorophyll *a* and turbidity was detected. In fact, out of the 11 input variables, turbidity was the only variable capable of significantly explaining parts of the observed variation in chlorophyll *a*. As shown on Figure 19A, 23 % of the variation in chlorophyll *a* could be explained by changes in turbidity. If the same correlation was repeated for non-log-transformed values (Figure 19B), this number dropped to 17 %, indicating a non-linear relationship between those two variables. Further results supporting this non-linear relationship will be presented in sub-chapter 5.6. If the extreme value of chlorophyll *a* would not have been excluded, the log-transformed data could explain 19% of chlorophyll *a* variation.

Despite the non-significant results of the other models presented in Figure 18, the direction of their modelled correlation can still be compared to the expected one. In the case of turbidity, glacier coverage, Glacial Index, conductivity and temperature, an agreement between our hypothesis and the results could be observed. However, for the very weak correlations the modelled correlation directions should not be overestimated, since in that case only few data points can have a large impact on the result.

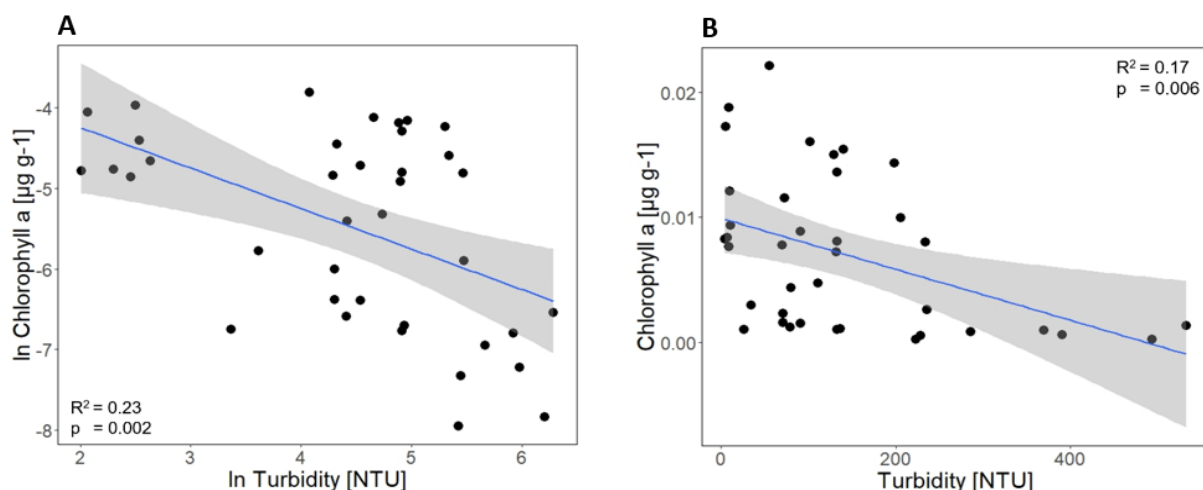


Figure 19 Correlation between turbidity and chlorophyll *a* using A) log-transformed B) and non-transformed data.

5.5.2 Multivariate linear regression

In a next step, I assessed whether multiple input variables together were capable of explaining the observed variation in chlorophyll a concentration. Despite the creation of many different subsets of non-collinear combinations of input variables (sub-chapter 4.5.3), the described variable selection process (sub-chapter 4.5.4) resulted in very few models that were overall significant and only contained variables which individually showed a significant correlation to chlorophyll a at a significance level of $p < 0.01$. Table 7 lists the three models that fulfill all these criteria.

Table 7 Best multivariate regression models explaining variation in chlorophyll a

Nr.	Variable 1	Coef. 1	Variable 2	Coef. 2	Variable 3	Coef. 3	p-value	adj. R ²
1	Turbidity	-0.56	Temperature	0.34	Surface Area	0.46	0.002	0.3
2	Turbidity	-0.61	Surface Area	0.35	Glacier Coverage	-1.4	0.003	0.27
3	Turbidity	-0.5					0.003	0.23

Strikingly, turbidity was consistently retained as the most influential factor in explaining chlorophyll a across sites. Model 1 and 2 both contained three components, including turbidity and surface area and are capable of explaining 30 % and 27 % of the variation in chlorophyll a, respectively. As a third component, model 1 included temperature, whereas model 2 included glacier coverage. Except for surface area, the slopes of all models correspond to the correlation directions that have been hypothesized based on glaciological and ecological reasoning.

Model 3 on the other hand, was the 1-component model described in the previous sub-chapter. According to its adjusted R² it can only explain 23 % of the variation in chlorophyll a, but it has the advantage of being a very simple model.

The following models (Table 8) were additional outcomes of the same methodological process, with slightly less strict selection criteria. During the process of creating possible combinations of non-collinear inputs, the variance inflation factors of <5 (instead of <3) were accepted.

All of them were 3- or 4-component models with similar or slightly higher adjusted R² than seen in the first three models. In addition to the model components seen before, additional variables include Glacial Index, Q_{abs} of the sampling month and snout distance. All four models included two variables each with partial slopes that did not correspond to the direction of correlation which was hypothesized (model 4 & 5: Q_{abs} sampling month & snout distance; model 6: surface area & snout

Table 8 Additional multivariate regression models explaining variation in chlorophyll a, based on less strict selection criteria

N	Variable 1	Coef. 1	Variable 2	Coef. 2	Variable 3	Coef. 3	Variable 4	Coef. 4	p-value	adj. R ²
4	Turbidity	-0.45	Temperature	0.5	Q _{abs} Sampl. Month	0.42	Snout Distance	-0.26	0.002	0.34
5	Turbidity	-0.58	Glacial Index	-6.22	Q _{abs} Sampl. Month	0.56	Snout Distance	-0.34	0.002	0.32
6	Turbidity	-0.62	Surface Area	0.65	Glacial Index	-6.1	Snout Distance	-0.34	0.002	0.3
7	Turbidity	-0.53	Temperature	-0.33	Q _{abs} Sampl. Month	0.39			0.001	0.3

5 Results

distance; model 7: temperature & Q_{abs}). It should be noted that model 1 and 7 are very similar, due to the high collinearity between surface area and Q_{abs} of the sampling month (Figure 8).

5.6 Potential threshold in turbidity controlling chlorophyll *a*

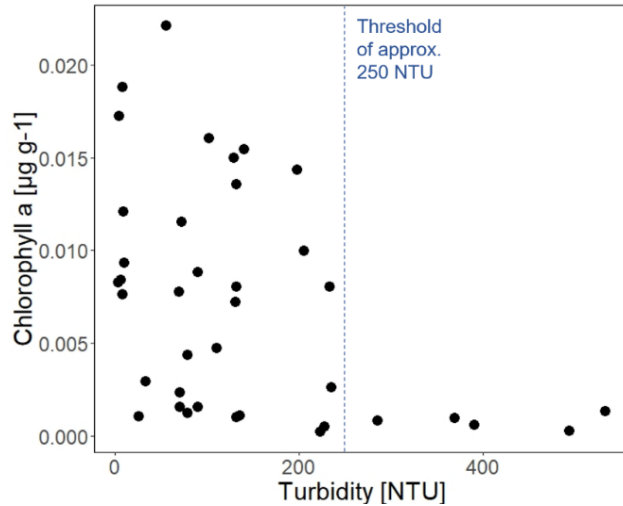


Figure 20 Potential turbidity threshold of approximately 250 NTU controlling chlorophyll *a* concentration.

While correlating the turbidity to chlorophyll *a*, it became apparent that in this case, the discovered association might not be a linear relationship. As visualized in Figure 20, above a potential threshold of approximately 250 NTU, virtually no chlorophyll *a* was observed (non-zero values were at the limit of detection). Below 250 NTU however, in some streams the chlorophyll *a* levels were still very low but in others, significantly higher concentrations have been detected.

Based on this observation, simple linear regression was repeated by only including the 33 observations with turbidity <250 NTU. In that case, the correlation was not significant and adj. R^2 dropped to 0.07, stating that turbidity alone was not capable of explaining parts of the variation in chlorophyll *a* anymore. Multiple linear regression with the remaining observations was also attempted but due to a combination of reduced statistical power and large sampling bias in the correlation variable latitude, no significant and at the same time non-biased correlations could be established for the remaining observations.

6 Discussion

In this work, I bridged glaciological and ecological research to better understand the potential impacts of glaciers on algal biomass, an important ecological variable. In order to achieve this, GIS-derived and modelled glaciological variables were combined with *in situ* physicochemical measurements and measurements of chlorophyll a in 20 glacier-fed streams around the world. I then evaluated the various variables and their respective ability to predict chlorophyll a concentrations and compared them with a previously established index of glacial impact, the Glacial Index. Taken together, my work indicates that glaciers exhibit a dominant control on algal biomass in glacier-fed streams, probably driven by streamwater turbidity and its impact on light availability. This extends previous knowledge and may guide us to the formulation of a revised Glacial Index.

6.1 Performance of the Glacial Index and potential alternatives to predict chlorophyll a

Of all the variables tested, Glacial Index showed the poorest performance in predicting chlorophyll a ($R^2 = 0.008$, $r = 0.03$, $p > 0.01$). Based on this dataset, no correlation between those two variables was detected, which differs from previous findings (Kohler and others 2020). In that study, samples of 20 glacier-fed streams in New Zealand taken and analyzed using identical protocols, showed a significant negative relationship between Glacial Index and chlorophyll a ($R^2 = 0.21$, $r = -0.46$, $p < 0.01$). However, in that case Glacial Index was not the best performing variable either; a much stronger correlation was detected for turbidity ($R^2 = 0.56$, $r = 0.75$, $p < 0.01$). Even though both datasets include 40 observations, they differ greatly in terms of uniformity. When only including samples from New Zealand instead of seven different field campaign destinations, the variance introduced by other potentially important characteristics (i.e. geological setting) can be expected to be substantially smaller, resulting in a clearer signal. Furthermore, in the New Zealand study, nearly the whole range of possible values of Glacial Index was represented (0.15 - 0.99), whereas the dataset analyzed here only contained values > 0.5 . Sites with hardly any glacial influence (i.e. $GI < 0.5$) might drive the correlation between Glacial Index and chlorophyll a. Hence, the two differing findings suggest to test this hypothesis again with a larger and global dataset, which will be possible in the course of the Vanishing Glaciers project. On the other hand, they both agree that other variables seem to be of greater importance than Glacial Index, which leads to the conclusion that alternatives to better predict chlorophyll a should be explored.

Before answering which combinations of glaciological and physicochemical stream variables best explain chlorophyll a values, in a first step, their individual performances in simple linear regression will be discussed. Even though the correlation with all variables except for turbidity were non-significant, they can still serve as a contribution to better understand the factors that potentially influence the ability of algae to grow in glacier-fed streams.

Turbidity is the best performing single variable ($R^2 = 0.23$, $r = -0.47$, $p < 0.01$; Figure 19) with an agreement between hypothesized and modelled direction of the correlation. As mentioned before, this observation is also in line with the one by Kohler and others (2020) and emphasizes the utility of this variable in explaining chlorophyll a patterns among glacier-fed streams. Sub-chapter 5.6 describes this correlation with a presumable threshold behavior in more detail.

Additional variables with coefficients matching the expected direction of the correlation were temperature, glacier coverage and conductivity. The weak positive correlation for temperature ($R^2 = 0.06$, $r = 0.25$, $p > 0.01$) indicates the appropriateness of the ecological hypothesis, but given that

glacier-fed streams are continuously cold, this surprisingly small influence of temperature might reflect the presence of well adapted cryospheric algal species. For both glacier coverage ($R^2 = 0.02$, $r = -0.15$) and conductivity ($R^2 = 0.01$, $r = 0.12$), the correlations were weak and insignificant in our dataset, and can be understood as an indication that the presumed ecological impact might be smaller than anticipated.

For the remaining variables, the analysis resulted in disagreement between hypothesized and modelled correlation direction. However, for the very weak correlations (snout distance, time since ice-free, Glacial Index and surface area) this direction should not be overestimated, since a few different data points could potentially reverse it.

For surface area ($R^2 = 0.0144$, $r = 0.12$) we expected a negative correlation, mainly due to the assumption that surface area acts as a surrogate for absolute discharge. This hypothesis seems to be too generalized both regarding the questions i) if larger glaciers really have larger absolute discharges (neglecting i.e. their aspect, debris cover, the surrounding topography and local climate) and ii) whether it can be stated that biofilm biomass is limited by higher absolute discharge alone, without any information on stream width or other streambed properties.

Neither the hypothesis about the snout distance nor time since ice-free was supported by the data. These two were very similar and might have hold true for sites either very far away from a glacier (presumably free of ice for a long time) or sites linked to nearly vanished glaciers with resulting lower discharges and reduced sediment transport. The majority of sampling sites however, are located above the respective Little Ice Age moraines and it can be assumed that the link between the glacier and its stream in terms of sediment transport and other potentially influential variables is still very strong in these locations. In other words, hypotheses that hold true for terrestrial plants cannot necessarily be applied to these complex aquatic ecosystems. Nevertheless, it would be interesting to explore potential non-linear trends using a larger dataset with a greater range in snout distance and ideally standardized distances or time periods, respectively.

A slightly stronger, positive correlation was indicated for latitude ($R^2 = 0.04$, $r = 0.2$). However, due to only few data points in low and high latitude, this correlation was biased. If the analysis was repeated with a more equal distribution of sampling sites across the latitude gradient, latitude could also act as a surrogate for other potentially important regional characteristics (i.e. geological setting).

Regarding the two discharge-related variables, a weak correlation has been detected for Q_{abs} sampling month ($R^2 = 0.03$, $r = 0.18$) and a slightly stronger one for CV of Q_{abs} ($R^2 = 0.08$, $r = 0.29$), both not corresponding to the expected correlation direction. Given that this data was derived from model predictions and consequently had low temporal resolution, our results indicate that this does not suffice to predict chlorophyll a concentrations in glacier-fed streams. This might not be surprising, given that sporadic precipitation events can lead to very rapid changes in discharge outweighing longer-term discharge dynamics. Such sporadic events, however, are not covered in terms of magnitude or frequency by the modeled data. Previous work on stream biofilms (Uehlinger and others, 2010) has highlighted the importance of such extreme events for benthic biomass and this seems to be similarly true for glacier-fed streams. In case of Q_{abs} sampling month it is probable that this information is not precise enough to reflect peaks in discharge a few days before sampling, which are likely to be more relevant. Hence, future work should focus on high-temporal resolution measures of predictions of discharge and investigate the timescale (including the magnitude, frequency, lags

between high flow events and biofilm recovery) to better understand the impacts of discharge on algal biomass in glacier-fed streams. Moreover, modelled data might also not be sufficient to accurately describe the small scale hydraulic conditions, which may depend on channel width and streambed characteristics. This notion is corroborated by the fact that, in the course of the field sampling, we sample copious biofilms from sheltered rocks. Hence, very small scale hydraulic conditions might be important to predict the patchy distribution of chlorophyll *a* in the streams. The weak correlation with CV of Q_{abs} , a measure of seasonal discharge variation, might be affected by similar issues. In this case it would probably have been much more crucial to be able to describe the flashiness of the discharge over the course of some days or weeks instead of over the course of the whole year, another sign of the limitations caused by the temporal resolution of the available input data.

To conclude the discussion about the performance of the individual variables in simple linear regression, it should be noted that all the measured physicochemical stream variables were capable of reflecting the hypothesized direction of the correlation, whereas for the majority of glaciological variables this was not the case. This might underscore the need of interdisciplinary work, crossing the borders between glaciology and stream ecology.

Regarding the question which combination of glaciological and physicochemical stream variables possess the highest power to explain measured chlorophyll *a* values, multivariate regression provides us with some answers. The aim of this analysis was clearly not to create a formula which can quantitatively predict chlorophyll *a* concentration (the dataset size was simply too small to achieve this goal in a robust manner), but rather to elaborate which combination of factors might play an important role in allowing or limiting algal growth. As seen in sub-chapter 5.5.2, out of seven models, the last four models (Table 8) were not only quite problematic from a collinearity point of view (regarding the accepted variance inflation factors of <5), but each one of them also contained two variables with partial slopes that didn't correspond to the underlying ecological hypothesis. Given the additional fact that these models were more complicated than the first three and hence less parsimonious, they were excluded from subsequent model selection.

Of the remaining three models, two retained glacier surface area, however with observed partial slopes of the regression not corresponding to the hypothesized direction. It is conceivable that surface area in this cases acted as a surrogate for another hidden common attribute of those glaciers (i.e. aspect, debris cover, altitude range, etc.) which has implications on algal growth. If one had to select between model 1 and 2, except for the slightly higher adj. R^2 of model 1, there are no other reasons to prefer one over the other, since the model components glacier coverage and temperature seem equally plausible. Model 3 on the other hand, has the great advantage of being an extremely simple 1-component model (turbidity alone) with a performance nearly comparable to the one of model 1 and 2.

The idea of revising the Glacial Index should be understood as the quest for combinations of variables that better explain observed chlorophyll *a* concentration than the Glacial Index for the purpose of monitoring but not for quantitative predictions. From the outcomes of multivariate regression, we can conclude that based on this dataset, the variables turbidity, glacial coverage (both negative correlations), as well as surface area and streamwater temperature (positive correlations) seem to be the most influential variables. Model 3 is the only one with a performance that can be confirmed based on other data, in this case from New Zealand. In both Kohler and others (2020) and in this analysis turbidity was an important determinant of chlorophyll *a* concentration and performed better in predicting chlorophyll *a* concentration than Glacial Index. Hence, streamwater turbidity, a

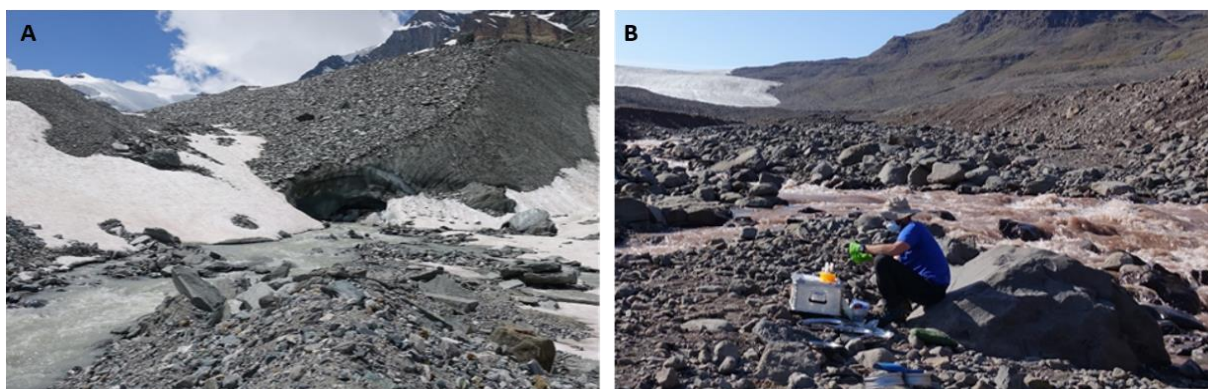
measurement that can be easily measured and included in monitoring efforts, should be considered as the best known alternative to Glacial Index. However, it is clear that turbidity also acts as a surrogate for multiple processes affecting benthic life in streams. Finally, more complicated indices are imaginable, but if they are based on the gradients represented in this dataset, most likely they will not bring any significant added value to the stream biofilm research community.

6.2 Interpretation of the observed threshold in turbidity

The observed potential threshold in turbidity (Figure 20) indicates that in waters above a turbidity level of appr. 250 NTU, it is hardly possible for phototrophic biofilm to survive. Photos 4 provide some visual examples of approximately these turbidity levels. As seen in sub-chapter 5.1, this observation matches very well with the hypotheses regarding limited light availability and its impacts on photosynthesis, as well as increased scouring due to a higher sediment load.

According to a study in the glacier-fed stream of Roseg Glacier (CH, part of our dataset, as well), in a water column of 0.5 m depth, a turbidity level of 250 NTU attenuated about 95 % of the incident light (Uehlinger and others, 2010). Our samples however, were taken at a water depth no larger than 0.2 m. Based on the findings of Lloyd (1987), an increase of 25 NTU is expected to reduce primary production by 13-50 %. By ‘shallow’ streams the authors refer to no more than 0.5 m water depth, which is a bit too vague to draw conclusions about the impact of 250 NTU on our samples. Nevertheless, these points indicate that reduced light availability due to high turbidity can act as an important limiting factor on primary production. To my knowledge, no previous studies have been conducted on streamwater turbidity and the associated damage of biofilm through scouring.

Below 250 NTU however, in some streams hardly any chlorophyll a was measured, either (Figure 20). This underlines the complexity of this ecosystem by showing that below such a threshold, other factors are important in controlling algal biomass. However, the statistical power of the remaining dataset after removing observations with turbidity >250 NTU was not high enough to better explore those factors. Since streamwater turbidity is a component of the habitat template that is expected to shift following the ‘peak water’ transition (Milner and others, 2017) it will be important to verify this observed threshold using a larger dataset.



Photos 4 Visual examples of turbidities of nearly 250 NTU: A) At the UP-site of Schwarzberg Glacier (CH) 206 NTU and B) at the DN-site of Chamberlin Glacier (GL) 228 NTU were measured.

6.3 Limitations and potential improvements of the research design

Based on the discussion above, it is clear that not a single variable determines the amount of algal biomass in any stream, and particularly not in glacier-fed streams. Hence, simple and multivariate regression analyses, which assume linear relationships underlying drivers and their interaction, might not adequately capture non-linear or threshold (e.g. such as the one suspected for turbidity) behaviors. Therefore, and given the small sample size, analyzing how this relations propagate beyond the available data range (i.e. extrapolations, space-for-time substitutions) were not attempted in this thesis. Moreover, each variable and the different procedures to estimate them involves various sources of uncertainties. Estimating uncertainties is a complex task ranging from field sampling routines (related to the fine-scale heterogeneity of the streambed), field and laboratory analyses (detection limits) to uncertainties related to statistical modeling. Some uncertainties have been implicitly addressed in the previous chapters, however, uncertainties will be further discussed in the next paragraphs followed by suggestions how to improve the research design in order to reduce them.

As seen in sub-chapter 5.2.1, the calculation of uncertainty according to the method described in Basnett and others (2013) revealed that for the variables surface area and glacier coverage, the error mainly results from interpretation uncertainty. The observed total mean error of 3.1% is in line with the results of a round robin experiment performed by Paul and others (2013). In their study, several experienced analysts were asked to manually map outlines of a selection of 24 glaciers multiple times. The sample contained a wide range of glacier sizes, clean and debris-covered glaciers and similar to my dataset, some were mapped based on high-resolution orthophotos and others based on satellite imagery with 30 m-resolution. Across all analysts and rounds of mapping, a standard deviation of 3.6% was observed. This confirms that the uncertainty of the mapped outlines corresponds to what is achievable using these data sources. According to the sensitivity analysis, the assumption that mapping based on orthophotos is more precise, could be validated. However, this assessment based on only three glaciers is not representative and was only performed to get a notion for the scales and sources of involved uncertainties.

Regarding the uncertainty of the timing of deglaciation, from a glaciological point of view, the results of glaciers reconstructed using method A) or B) (sub-chapter 4.2.2) seem quite robust. Nevertheless, if a sampling site became free of ice very recently, a maximal error bar length of six years seems still large in terms of stream ecological interpretation. For five sites the only option was to use method C), which is based on absolute values of front variation measured at the tip of the snout. However, some of the streams emerge from the lateral ice margin, which might have also impacted the accuracy of the result. It will be interesting to understand if variation on such short time-scales (few years or decades) matter for the dynamics of algal growth in glacier-fed streams. This is an important research question, particularly if the rate of succession would not keep up with the rapid recession of glaciers.

Compared to the glaciological variables, the uncertainty and representativeness of chlorophyll a and the measured field variables are more difficult to quantify. As outlined in sub-chapters 2.1 and 2.2, these variables underlie seasonal and the latter also diurnal fluctuations and hence, the measurements have to be regarded as snapshots that come along with the logistical and time constraints of such a large, global research project. Regarding the seasonality of the chlorophyll a concentration, we aimed to sample all glaciers as close to the peak of the respective ablation season as possible. As indicated

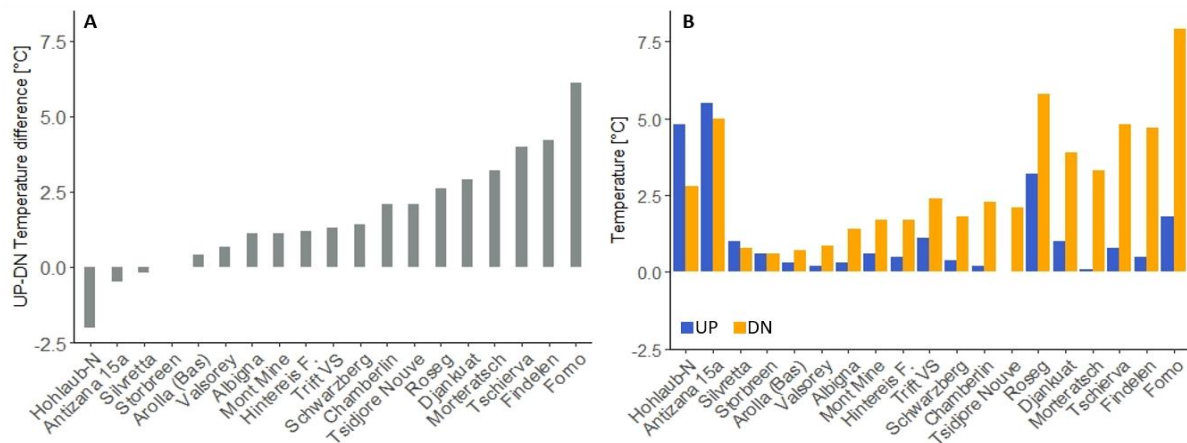


Figure 21 A) UP- to DN-site differences in temperature and B) temperatures at UP-vs. DN sites.

by the large intra-site variability (Figure 16), chlorophyll a also shows a large spatial variability. This patchiness can easily be explained by the inhomogeneous distribution of sediment biofilm due to variable hydraulic conditions and the dynamic nature of the stream bed (Allan and others, 2021). If instead of sediment biofilm, we would have sampled rock biofilm, perhaps slightly more uniform results might have been measured. These habitats are expected to be more stable and allow for a longer time to develop biomass and reach equilibrium with their environment (H. Peter, pers. comm.). The fact that this study is based on sediment biofilm (sub-chapter 3.2) introduced the additional challenge, that due to the invisible nature of this type of biofilm, no direct observations can be made in the field. In other words, the learning effect during many hours of field work is limited to the observations of the other variables and at this moment, the representativeness of a sampling site cannot be assessed.

Furthermore, the uncertainty regarding temporal and spatial variability of the measured stream variables deserves some discussion. All three variables are based on point measurements as described in sub-chapter 4.4.2. Temperature fluctuates in seasonal and diurnal patterns (Uehlinger and others, 2010). Since the sampling day for chlorophyll a analysis corresponds to the one of the temperature measurements and due to the unknown residence time of sediment and associated biofilm, diurnal variations are probably more important to consider. The shorter the distance between sampling site and glacier snout, the less pronounced are these fluctuations expected to be, due to the constant input of 0 °C melt water (Brown and others, 2003). For all the glaciers, the measurements at the DN-sites were performed 3 - 4 h after the ones at the UP-sites, which introduces a sampling bias. The UP- vs. DN-site temperature differences (Figure 21A) show that in almost every stream, temperature increased downstream. However, the significant positive correlation between temperature and snout distance ($R^2 = 0.34$, $r = 0.58$) indicates that a large part of this temperature difference can be attributed to the downstream warming of the meltwater (the reason why none of the variable combinations for multivariate regression contained both snout distance and temperature). Even though the variable temperature is based on a point measurement, we simultaneously conducted another field experiment (ecosystem respiration), where temperature was continuously measured for 2 h. This data shows that within 2 h, on average, temperature fluctuated at UP sites by only 1.35°C and at DN sites by 1.58°C. This supports the notion that temperature differences between UP and DN sites that averaged 1.7°C result from longitudinal changes in temperature rather than from changes during the day. Hence, the point measurements should be able to reflect the temperature variability between

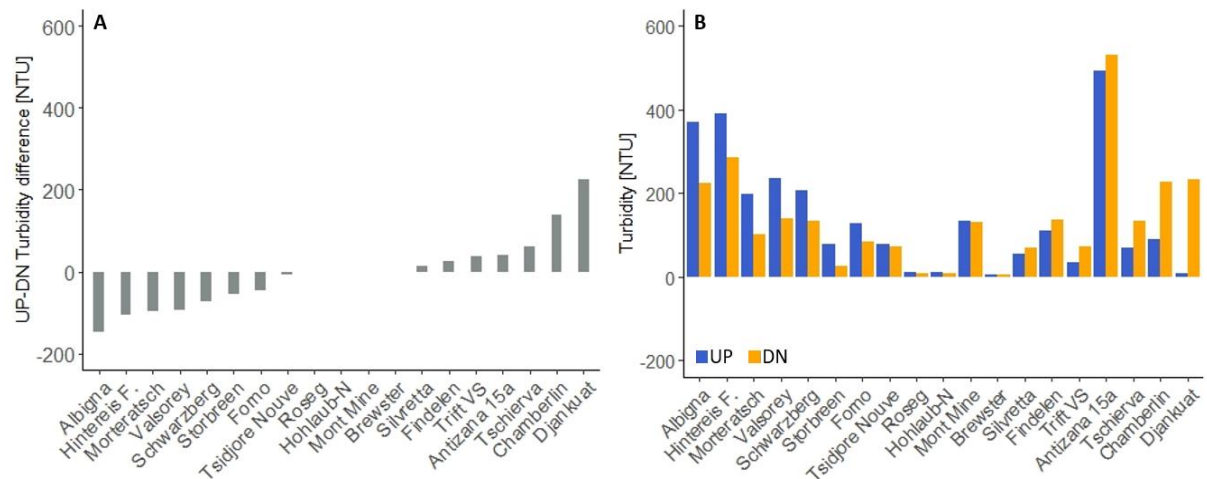


Figure 22 UP- to DN- site differences in turbidity and B) UP- vs. DN-site turbidity levels.

different glacier-fed streams and sites controlled by factors like snout distance, flow velocity, water depth or albedo of the stream bed, rather than sampling time.

In terms of conductivity, UP- vs. DN-site measurements showed very similar results, suggesting a remarkable stability in streamwater chemistry. For turbidity on the other hand, an equal amount of negative and positive gradients was observed (Figure 22). The latter could be attributed to increased discharge in the course of the sampling day, whereas a negative gradients might be interpreted as a result of increased downstream mixing of turbid glacier water with ground water. Unfortunately, the variability of turbidity is much more complex and includes stochastic factors (Benn and Evans, 2013). Even though marked diurnal fluctuations in sediment concentrations have been related to the discharge regime, suspended sediment concentrations can suddenly change at the scale of hours without any significant change in discharge (reviewed in Clifford and others, 1995). Such brief pulses of suspended sediment can be caused i.e. by the collapse of a melt channel wall or changes in the channel patterns (Benn and Evans, 2013). Hence, conducting more representative turbidity measurements would be very time consuming. Nevertheless, as a potential improvement, the time span of the 2 - 3 h we spend at each sampling site, could be used for continuous measuring. However, the inter-site variability (up to 528 NTU, Figure 22B) was much more pronounced than the maximal UP- vs. DN-site variability of 224 NTU. This indicates that contrasts in a number of factors including underlying rock type (Photo 5) and subglacial deposits, rates of glacier movement, character of the glacier drainage system as well as topography of the catchment (Gurnell and others, 1996) are influential on a global scale.

Reflecting on potential improvements of the research design resulted in several suggestions that are linked to the fact, that the sampling design was not originally planned for this thesis, but for the Vanishing Glaciers

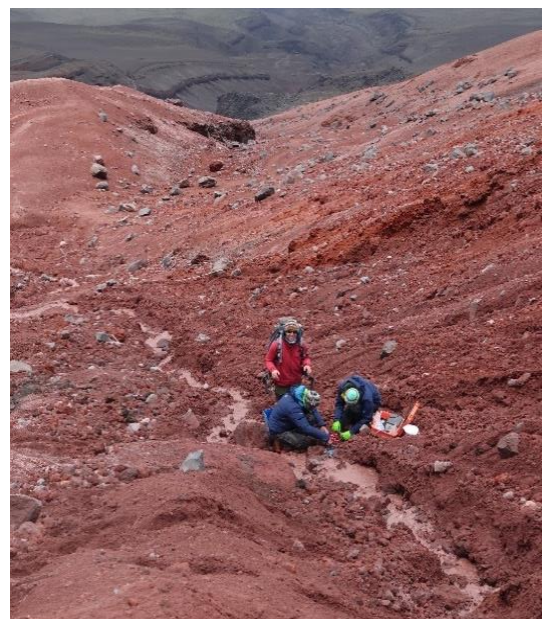


Photo 5 A sampling site on the Cotopaxi Volcano (EC, with similar characteristics like the stream of Antizana 15a), illustrating the pronounced differences in geological setting and topography, i.e. compared to the to the European Alps.

project. However, even in this framework, all three physicochemical stream variables could be measured continuously during the 2-3 h time interval the field team spends working at one sampling site. If I was to conduct again a study about the influence of discharge on chlorophyll a, I would select the sampling locations in a way that enables me to work with measured instead of modelled data. Such data would allow to include more precise and potentially more influential discharge variables like the timespan between the last major peak in discharge and the moment of sampling. Obviously, suitable streams with nearby gauging stations are very rare and such a choice would greatly impact the possible geographical scope of the study.

Regarding the choice of the sampling locations, it could be very interesting to include sites that extend the maximal gradient for instance in Glacial Index. However, depending on the catchment characteristics, it can be very challenging to find such locations that fulfill these requirement, but are not impacted by additional water input from other sources.

An idea to model incoming solar radiation at the specific stream site in GIS had to be abandoned due to technical problems regarding computing power and resulting time constraints. This could still be a very interesting variable to investigate, but the modelling would need to be combined with measurements on light attenuation depending on turbidity and water depth, to estimate how much light actually reaches the streambed.

If I was to deepen the understandings of the complex interactions in this ecosystem even more, I would try to additionally gain a better understanding about the role of available nutrients and the potential impacts of predators on algal biomass.

Two potential improvements don't specifically relate to the uncertainty but simply to the efficiency of the glacier mapping work flow. The use of Google Earth Engine (<https://earthengine.google.com/>) can save a large amount of time while searching for ideal satellite scenes with good contrast and minimal seasonal snow cover. Furthermore, the manual mapping of the catchment can be replaced by a combined approach of automatic delineation for catchments where the algorithms perform well and manual delineation in the case of the remaining ones. Meanwhile, these two methodological improvements have already been successfully implemented in the GIS analysis for the Vanishing Glaciers project.

7 Conclusions and Outlook

According to this dataset, Glacial Index shows a poor performance in predicting chlorophyll a. Even though this is not in line with the findings of Kohler and others (2020), both studies agree that the observed chlorophyll a concentrations can be better explained by stream water turbidity. Furthermore, this study suggests a potential threshold behavior of turbidity in controlling chlorophyll a concentration. As shown by the results of multivariate regression modelling, more complex indices to predict chlorophyll a are imaginable. But based on the observed variable gradients and the representativity of this dataset, they will most likely not bring a significant added value to the stream biofilm research community.

Due to the complex environmental interactions in the glacier-fed stream ecosystem, detected correlations were relatively weak, which is not unusual in the field of ecology. If the uncertainties associated with a sampling concept not specifically designed for this study could be reduced and larger variable gradients would be included, stronger correlations might be observed.

To fulfill the aim of this thesis, glaciology and stream ecology knowledge was combined and hypotheses that so far were just assumed to be true, were quantitatively tested. While doing so, the absence of a correlation contributed equally to a better understanding of the ecological interactions. Furthermore, having tested the methods to calculate these glaciological variables, as well as the reflection about their limitations will certainly contribute to the Vanishing Glaciers project. For research questions related to microbial diversity and adaptation to this harsh ecosystem, some of these variables might prove to be quite influential. Moreover, the whole process clearly showed the numerous challenges associated with interdisciplinary research, as well as the fascinating aspects of such an approach to study the complex and interconnected impacts of glaciers on the stream ecosystem.

Given the two differing conclusions on the performance of the Glacial Index as a predictor of chlorophyll a, this hypothesis should be retested. It seems plausible that across a rather homogenous dataset like the one from New Zealand, Glacial Index as a rough estimate of environmental harshness manages to explain parts of the variation in chlorophyll a concentration. For a more heterogenous selection of stream ecosystems on the other hand, a predictor with a much more direct impact on biofilm like turbidity, might be needed. This hypothesis can only be tested with a larger dataset. Furthermore, the potential threshold in turbidity might be an exciting finding but also needs to be validated based on more representative data. Since turbidity levels are expected to shift following the peak water transition (Milner and others, 2017), it is crucial to better understand their implications on biofilm, as well as the associated downstream consequences.

8 References

- Abrams M and Crippen R** (2019) ASTER GDEM V3 (ASTER Global DEM). User guide. https://lpdaac.usgs.gov/documents/434/ASTGTM_User_Guide_V3.pdf.
- Abrams M, Hook S and Ramachandran B** (2002) ASTER user handbook. *Pasadena, CA: Jet Propulsion Laboratory*, 45–54.
- Allan JD, Castillo MM and Capps KA** (2021) *Stream Ecology: Structure and Function of Running Waters*. Springer International Publishing, Cham. doi:10.1007/978-3-030-61286-3.
- BAFU** (2021) Topographische Einzugsgebiete Schweizer Gewässer. Accessed 25 July 2020, <https://www.bafu.admin.ch/bafu/de/home/themen/thema-wasser/wasser--daten--indikatoren-und-karten/wasser--geodaten-und-karten/einzugsgebietsgliederung-schweiz.html>.
- Basnett S, Kulkarni AV and Bolch T** (2013) The influence of debris cover and glacial lakes on the recession of glaciers in Sikkim Himalaya, India. *Journal of Glaciology* **59**(218), 1035–1046. doi:10.3189/2013JoG12J184.
- Battin TJ, Besemer K, Bengtsson MM, Romani AM and Packmann AI** (2016) The ecology and biogeochemistry of stream biofilms. *Nature Reviews Microbiology* **14**(4), 251–263. doi:10.1038/nrmicro.2016.15.
- Benn DI and Evans DJA** (2013) *Glaciers & glaciation.*, 2. ed. Routledge, London.
- Bernhardt ES and 13 others** (2018) The metabolic regimes of flowing waters: Metabolic regimes. *Limnology and Oceanography* **63**(S1), S99–S118. doi:10.1002/lno.10726.
- Besemer K and 6 others** (2012) Unraveling assembly of stream biofilm communities. *The ISME Journal* **6**(8), 1459–1468. doi:10.1038/ismej.2011.205.
- Bolch T, Menounos B and Wheate R** (2010) Landsat-based inventory of glaciers in western Canada, 1985–2005. *Remote sensing of Environment* **114**(1), 127–137. doi: 10.1016/j.rse.2009.08.015.
- Brown LE and 18 others** (2018) Functional diversity and community assembly of river invertebrates show globally consistent responses to decreasing glacier cover. *Nature Ecology & Evolution* **2**(2), 325–333. doi:10.1038/s41559-017-0426-x.
- Brown LE, Hannah DM and Milner AM** (2003) Alpine Stream Habitat Classification: An Alternative Approach Incorporating the Role of Dynamic Water Source Contributions. *Arctic, Antarctic, and Alpine Research* **35**(3), 313–322. doi:10.1657/1523-0430(2003)035[0313:ASHCAA]2.0.CO;2.
- Brown LE, Hannah DM and Milner AM** (2007) Vulnerability of alpine stream biodiversity to shrinking glaciers and snowpacks. *Global Change Biology* **13**(5), 958–966. doi:10.1111/j.1365-2486.2007.01341.x.
- Brown JH, Gillooly JF, Allen AP, Savage VM and West GB** (2004) Toward a metabolic theory of ecology. *Ecology* **85**(7), 1771–1789. doi: 10.1890/03-9000.
- Cano-Paoli K, Chiogna G and Bellin A** (2019) Convenient use of electrical conductivity measurements to investigate hydrological processes in Alpine headwaters. *Science of The Total Environment* **685**, 37–49. doi:10.1016/j.scitotenv.2019.05.166.

- Cauvy-Fraunié S, Andino P, Espinosa R, Calvez R, Jacobsen D and Dangles O** (2016) Ecological responses to experimental glacier-runoff reduction in alpine rivers. *Nature Communications* **7**(1), 12025. doi:10.1038/ncomms12025.
- Clifford NJ, Richards KS, Brown RA and Lane SN** (1995) Scales of Variation of Suspended Sediment Concentration and Turbidity in a Glacial Meltwater Stream. *Geografiska Annaler*, **22**. doi: 10.1080/04353676.1995.11880428.
- Davies-Colley RJ and Smith DG** (2001) Turbidity, suspended Sediment, and Water Clarity: A Review. *Journal of the American Water Resources Association* **37**(5), 1085–1101. doi:10.1111/j.1752-1688.2001.tb03624.x.
- Elser JJ and 27 others** (2020) Key rules of life and the fading cryosphere: Impacts in alpine lakes and streams. *Global Change Biology* **26**(12), 6644–6656. doi:10.1111/gcb.15362.
- Ernste H** (2011) *Angewandte Statistik in Geografie und Umweltwissenschaften*. vdf Hochschulverlag AG, Zürich.
- ESA** (2021) User Guides - Sentinel-2 MSI - Overview - Sentinel Online - Sentinel. Accessed May 15 2021, <https://sentinel.esa.int/web/sentinel/user-guides/sentinel-2-msi/overview>.
- Falkowski PG and Raven JA** (2013) *Aquatic photosynthesis*. Princeton University Press, Princeton.
- Flemming H-C and Wingender J** (2010) The biofilm matrix. *Nature reviews microbiology* **8**(9), 623–633. doi: 10.1038/nrmicro2415.
- Gardner AS and 15 others** (2013) A reconciled estimate of glacier contributions to sea level rise: 2003 to 2009. *science* **340**(6134), 852–857. doi: 10.1126/science.1234532.
- Garmin** (2021) GPS Accuracy | Garmin Support. Accessed May 12 2021, <https://support.garmin.com/en-US/?faq=aZc8RezeAb9LjCDpJpITY7>.
- Gurnell A, Hannah D and Lawler D** (1996) Suspended sediment yield from glacier basins. *IAHS Publications-Series of Proceedings and Reports-Intern Assoc Hydrological Sciences* **236**, 97–104.
- Hugonnet R and 10 others** (2021) Accelerated global glacier mass loss in the early twenty-first century. *Nature* **592**(7856), 726–731. doi:10.1038/s41586-021-03436-z.
- Huss M and Hock R** (2015) A new model for global glacier change and sea-level rise. *Frontiers in Earth Science* **3**. doi:10.3389/feart.2015.00054.
- Huss M and Hock R** (2018) Global-scale hydrological response to future glacier mass loss. *Nature Climate Change* **8**(2), 135–140. doi:10.1038/s41558-017-0049-x.
- Ilg C and Castella E** (2006) Patterns of macroinvertebrate traits along three glacial stream continuums. *Freshwater Biology* **51**(5), 840–853. doi:10.1111/j.1365-2427.2006.01533.x.
- Jacobsen D and Dangles O** (2012) Environmental harshness and global richness patterns in glacier-fed streams: Harshness and richness in glacier-fed streams. *Global Ecology and Biogeography* **21**(6), 647–656. doi:10.1111/j.1466-8238.2011.00699.x.
- Jacobsen D, Milner AM, Brown LE and Dangles O** (2012) Biodiversity under threat in glacier-fed river systems. *Nature Climate Change* **2**(5), 361–364. doi:10.1038/nclimate1435.

8 References

- Kassambara A** (2021) Best Subsets Regression Essentials in R - Articles - STHDA. *Model selection Essentials in R*. Accessed June 05 2021, <http://www.sthda.com/english/articles/37-model-selection-essentials-in-r/155-best-subsets-regression-essentials-in-r/>.
- Kohler TJ and 11 others** (2020) Patterns and Drivers of Extracellular Enzyme Activity in New Zealand Glacier-Fed Streams. *Frontiers in Microbiology* **11**, 591465. doi:10.3389/fmicb.2020.591465.
- Lencioni V** (2018) Glacial influence and stream macroinvertebrate biodiversity under climate change: Lessons from the Southern Alps. *Science of The Total Environment* **622–623**, 563–575. doi:10.1016/j.scitotenv.2017.11.266.
- Łepkowska E and Stachnik Ł** (2018) Which Drivers Control the Suspended Sediment Flux in a High Arctic Glacierized Basin (Werenskioldbreen, Spitsbergen)? *Water* **10**(10), 1408. doi: 10.3390/w10101408.
- Lloyd DS** (1987) Turbidity as a water quality standard for salmonid habitats in Alaska. *North American journal of fisheries management* **7**(1), 34–45. doi: 10.1577/1548-8659(1987)7 <34:TAAWQS> 2.0.CO;2.
- Milner AM, Brown LE and Hannah DM** (2009) Hydroecological response of river systems to shrinking glaciers. *Hydrological Processes* **23**(1), 62–77. doi:10.1002/hyp.7197.
- Milner AM and 16 others** (2017) Glacier shrinkage driving global changes in downstream systems. *Proceedings of the National Academy of Sciences* **114**(37), 9770–9778. doi:10.1073/pnas.1619807114.
- Milner AM and Petts GE** (1994) Glacial rivers: physical habitat and ecology. *Freshwater Biology* **32**(2), 295–307. doi: 10.1111/j.1365-2427.1994.tb01127.x.
- NASA** (2021) Sentinel-2 - Missions - Sentinel Online - Sentinel. Accessed May 12 2021, <https://sentinel.esa.int/web/sentinel/missions/sentinel-2>.
- NASA, METI, AIST, Japan Space Systems and U.S./Japan ASTER Science Team et al.** (2019) ASTER Global Digital Elevation Model V003. doi:10.5067/ASTER/ASTGTM.003.
- Odum E and Barrett GW** (2004) Fundamentals of ecology. cengage learning, Boston, US.
- Paul F and 9 others** (2009) Recommendations for the compilation of glacier inventory data from digital sources. *Annals of Glaciology* **50**(53), 119–126. doi:10.3189/172756410790595778.
- Paul F and 19 others** (2013) On the accuracy of glacier outlines derived from remote-sensing data. *Annals of Glaciology* **54**(63), 171–182. doi: 10.3189/2013AoG63A296.
- Paul F and 24 others** (2015) The glaciers climate change initiative: Methods for creating glacier area, elevation change and velocity products. *Remote Sensing of Environment* **162**, 408–426. doi:10.1016/j.rse.2013.07.043.
- Pfankuch DJ** (1975) Stream reach inventory and channel stability evaluation. USDA Forest Service. Washington DC, US Government Printing Office (696), 26.
- Pfeffer WT and 19 others** (2014) The Randolph Glacier Inventory: a globally complete inventory of glaciers. *Journal of glaciology* **60**(221), 537–552. doi: 10.3189/2014JoG13J176.
- Quincey DJ and 13 others** (2014) Digital terrain modeling and glacier topographic characterization. *Global land ice measurements from space*. Springer, 113–144.

- Raup B and Khalsa SJS** (2010) GLIMS analysis tutorial. *Boulder, CO: National Snow*.
- Raup B, Racoviteanu A, Khalsa SJS, Helm C, Armstrong R and Arnaud Y** (2007) The GLIMS geospatial glacier database: a new tool for studying glacier change. *Global and Planetary Change* **56**(1–2), 101–110. doi: 10.1016/j.gloplacha.2006.07.018.
- Ren Z, Martyniuk N, Oleksy IA, Swain A and Hotaling S** (2019) Ecological Stoichiometry of the Mountain Cryosphere. *Frontiers in Ecology and Evolution* **7**, 360. doi:10.3389/fevo.2019.00360.
- Roncoroni M, Brandani J, Battin TI and Lane SN** (2019) Ecosystem engineers: Biofilms and the ontogeny of glacier floodplain ecosystems. *WIREs Water* **6**(6). doi:10.1002/wat2.1390.
- Sommaruga R** (2015) When glaciers and ice sheets melt: consequences for planktonic organisms. *Journal of Plankton Research* **37**(3), 509–518. doi:10.1093/plankt/fbv027.
- swisstopo** (2018) swissALTI3D Das hoch auf-gelöste Terrainmodell der Schweiz. Accessed May 17 2021, <https://www.swisstopo.admin.ch/de/geodata/height/alti3d.html#dokumente>.
- swisstopo** (2020) SWISSIMAGE Das digitale Orthophotomosaik der Schweiz. Accessed May 17 2021, file:///C:/Users/schoen/AppData/Local/Temp/Produktinfo_SWISSIMAGE10cm_DE_bf.pdf.
- swisstopo** (2021a) Swiss Geoportal. *geo.admin.ch*. Accessed May 17 2021, <https://map.geo.admin.ch>.
- swisstopo** (2021b) Swiss Map Raster 25. Accessed May 17 2021, <https://www.swisstopo.admin.ch/de/geodata/maps/smr/smr25.html>.
- swisstopo** (2021c) Background information on the Dufour Map., *Federal Office of Topography swisstopo*. Accessed May 18 2021, <https://www.swisstopo.admin.ch/en/knowledge-facts/histcoll/historical-maps/dufour-map.html>.
- swisstopo** (2021d) Background information on the Siegfried Map. *Federal Office of Topography swisstopo*. Accessed May 18 2021, <https://www.swisstopo.admin.ch/en/knowledge-facts/histcoll/historical-maps/siegfried-map.html>.
- swisstopo** (2021e) Background information on the National Map. *Federal Office of Topography swisstopo*. Accessed May 18 2021, <https://www.swisstopo.admin.ch/en/knowledge-facts/histcoll/historical-maps/national-map.html>.
- swisstopo** (2021f) Historical maps. *Federal Office of Topography swisstopo*. Accessed May 17 2021, <https://www.swisstopo.admin.ch/en/knowledge-facts/histcoll/historical-maps.html>.
- Taylor KE, Stouffer RJ and Meehl GA** (2012) An overview of CMIP5 and the experiment design. *Bulletin of the American meteorological Society* **93**(4), 485–498. doi: 10.1175/BAMS-D-11-00094.1.
- Uehlinger U, Kawecka B and Robinson CT** (2003) Effects of experimental floods on periphyton and stream metabolism below a high dam in the Swiss Alps (River Spöl). *Aquatic Sciences* **65**(3), 199–209. doi: 10.1007/s00027-003-0664-7.
- Uehlinger U, Robinson CT, Hieber M and Zah R** (2010) The physico-chemical habitat template for periphyton in alpine glacial streams under a changing climate. *Hydrobiologia* **657**(1), 107–121. doi:10.1007/s10750-009-9963-x.

8 References

- Ward JV** (1994) Ecology of alpine streams. *Freshwater biology* **32**(2), 277–294. doi: 10.1111/j.1365-2427.1994.tb01126.x.
- Welschmeyer NA** (1994) Fluorometric analysis of chlorophyll a in the presence of chlorophyll b and pheopigments. *Limnology and Oceanography* **39**(8), 1985–1992. doi:10.4319/lo.1994.39.8.1985.
- WGMS** (2012) Fluctuations of Glaciers 2005-2010 (Vol. X): Zemp, M., Frey, H., Gärtner-Roer, I., Nussbaumer, S.U., Hoelzle, M., Paul, F. & W. Haeberli (eds.), ICSU (WDS)/ IUGG (IACS)/ UNEP/ UNESCO/ WMO, World Glacier Monitoring Service, Zurich, Switzerland. Based on database version doi: 10.5904/wgms-fog-2012-11.
- WGMS** (2019) Fluctuations of Glaciers Database. World Glacier Monitoring Service, Zurich, Switzerland. doi:10.5904/WGMS-FOG-2019-12. Online access: <http://dx.doi.org/10.5904/wgms-fog-2019-12>.
- WGMS** (2020) Global Glacier Change Bulletin No. **3** (2016–2017). Zemp M, Gärtner-Roer I, Nussbaumer SU, Bannwart J, Rastner P, Paul F, Hoelzle M, editors. Zurich, Switzerland: ISC (WDS) / IUGG (IACS) / UNEP / UNESCO / WMO, World Glacier Monitoring Service. Publication based on database version: doi:10.5904/wgms-fog-2019-12.
- Wilhelm L, Singer GA, Fasching C, Battin TJ and Besemer K** (2013) Microbial biodiversity in glacier-fed streams. *The ISME Journal* **7**(8), 1651–1660. doi:10.1038/ismej.2013.44.
- Zemp M and 38 others** (2015) Historically unprecedented global glacier decline in the early 21st century. *Journal of glaciology* **61**(228), 745–762. doi: 10.3189/2015JoG15J017.
- Zemp M and 14 others** (2019) Global glacier mass changes and their contributions to sea-level rise from 1961 to 2016. *Nature* **568**(7752), 382–386. doi: 10.1038/s41586-019-1071-0.
- Zuur AF, Ieno EN and Elphick CS** (2010) A protocol for data exploration to avoid common statistical problems: *Data exploration. Methods in Ecology and Evolution* **1**(1), 3–14. doi:10.1111/j.2041-210X.2009.00001.x.

Appendix

A. Methods

Sensitivity analysis of the mapped glacier outlines

Appendix 1 Four mini-inventories comprising glacier surface area, catchment area and glacier coverage based on different combinations of data sources. The approach of this uncertainty assessment is explained in detail in sub-chapter 4.1.3.

Inventory A (Sentinel & high resolution catchment)

Glacier Name	Surface Area	Catchment area	Glacier coverage
Findelen	15.36	20.66	74%
Schwarzberg	6.34	8.13	78%
Silvretta	2.41	3.50	69%

Inventory B (Swissimage & high resolution catchment)

Glacier Name	Surface Area	Catchment area	Glacier coverage
25	15.38	20.66	74.5%
31	5.84	8.13	72%
82	2.36	3.50	67%

Inventory C (Swissimage & medium resolution catchment)

Glacier Name	Surface Area	Catchment area	Glacier coverage
Findelen	15.37	20.43	75.2%
Schwarzberg	5.70	8.68	65.6%
Silvretta	2.32	3.42	68.0%

Inventory D (Sentinel & medium resolution catchment)

Glacier Name	Surface Area	Catchment area	Glacier coverage
25	15.21	20.43	74.4%
31	6.40	8.68	73.7%
82	2.36	3.42	69.0%

Appendix 2 Sensitivity of selected glaciological variables to the image resolution, the DEM resolution and to the combined impact of the image and DEM resolution.

1. A vs. B (Impact of image resolution -> Sentinel vs. Swissimage)

	Δ Surface Area	Δ Catchment Area	Δ Glacier Coverage
Findelen	0.02		0.001
	0.1%		0.1%
Schwarzberg	-0.51		-0.06
	-8.9%		-9.5%
Silvretta	-0.05		-0.01
	-2.3%		-2.2%
Average	-0.18		-0.03
	-3.7%		-3.9%

2. B vs. C (Impact of DEM resolution -> Alti3d vs. Aster)

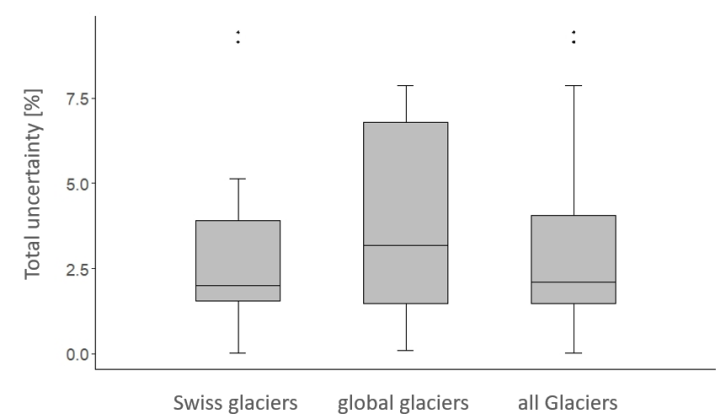
	Δ Surface Area	Δ Catchment Area	Δ Glacier Coverage
Findelen	0.01	0.22	-0.01
	0.1%	1.1%	-1.0%
Schwarzberg	0.14	-0.55	0.06
	2.4%	-6.8%	8.6%
Silvretta	0.04	0.09	-0.006
	1.5%	2.4%	-1.0%
Average	0.1	-0.1	0.02
	1.3%	-1.1%	2.2%

3. B vs D (Combined impact of image and DEM resolution)

	Δ Surface Area	Δ Catchment Area	Δ Glacier Coverage
Findelen	0.17		0.0003
	1.1%		0.0%
Schwarzberg	-0.56		-0.02
	-10%		-2.7%
Silvretta	0.00		-0.02
	0%		-2.5%
Average	-0.13		-0.01
	-2.8%		-1.7%

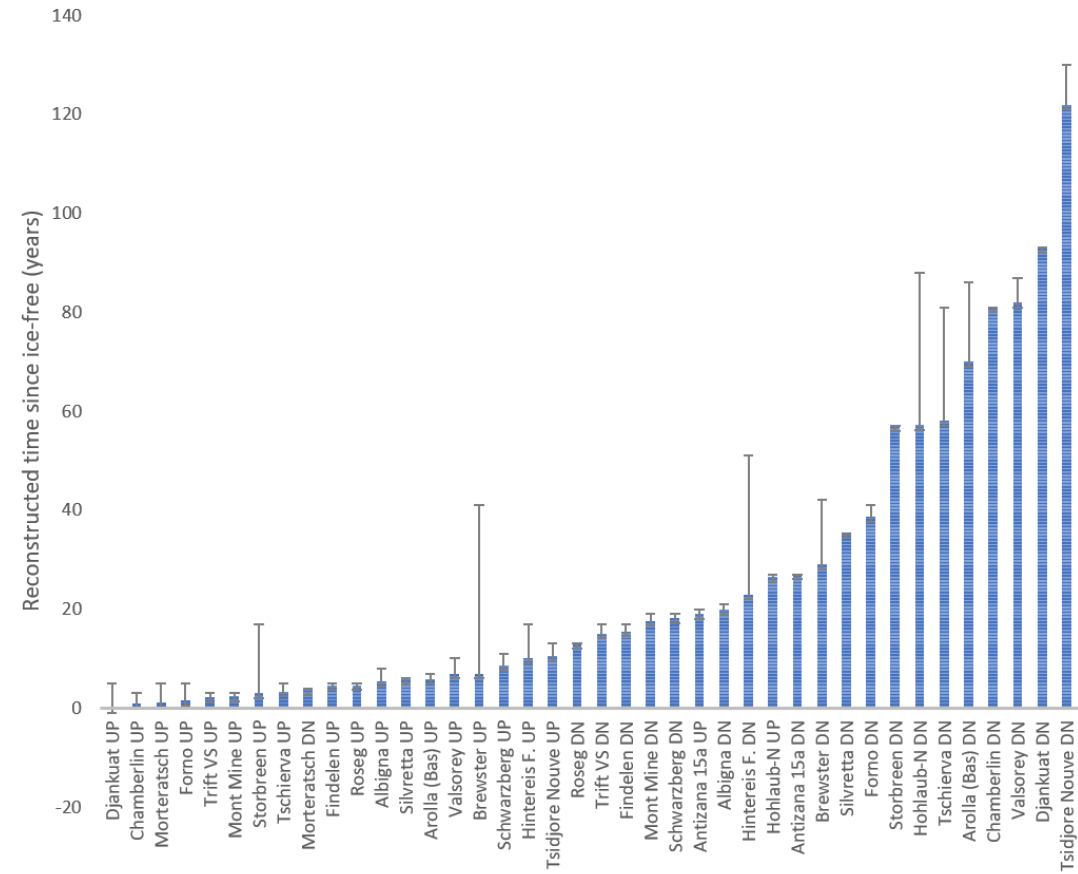
8 References

Assessment of the mapping and interpretation uncertainty of the glacier outlines



Appendix 3 Results of uncertainty assessment based on the method recommended by Basnett and others (2013, sub-chapter 4.1.3). Higher uncertainties were observed for the mapped outlines of the global glaciers compared to the Swiss ones.

Deglacierization analysis



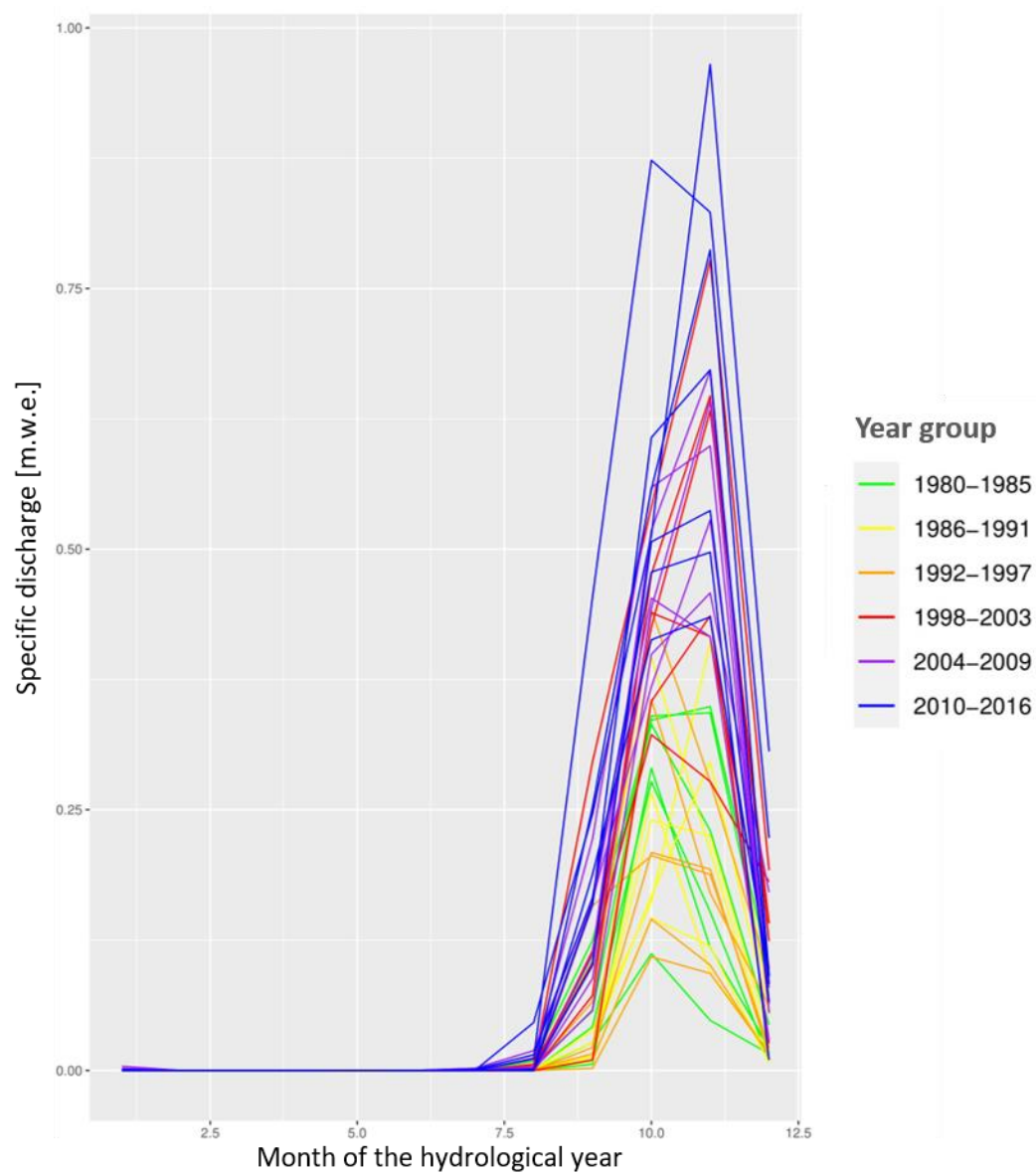
Appendix 4 Estimated amount of years the sampling sites have been free of ice. The error bars refer to the years of the known glacier extents and therefore represent the most pessimistic scenario in terms of reconstruction uncertainty.

Appendix 5 Overview of the methods used for the reconstruction of the timing of deglaciation including the results and corresponding uncertainty.

Sampling site name	Reconstruction Method	Time since ice-free [years]	Length of error bar [years]
Djankuat UP	A	0.0	5
Chamberlin UP	A	1.0	3
Morteratsch UP	A	1.0	4
Forno UP	A	1.5	4
Trift VS UP	A	2.2	3
Mont Mine UP	A	2.4	3
Storbreen UP	B	3.0	17
Tschierva UP	A	3.3	4
Morteratsch DN	A	3.7	4
Findelen UP	A	4.6	2
Roseg UP	A	4.6	4
Albigna UP	A	5.4	3
Silvretta UP	A	5.8	1
Arolla (Bas) UP	A	5.9	2
Valsorey UP	A	7.0	3
Brewster UP	B	7.0	38
Schwarzberg UP	A	8.6	3
Hintereis F. UP	B	10.0	17
Tsidjore Nouve UP	A	10.6	3
Roseg DN	A	13.0	3
Trift VS DN	A	15.1	2
Findelen DN	A	15.5	2
Mont Mine DN	A	17.6	2
Schwarzberg DN	A	18.1	4
Antizana 15a UP	B	19.0	19
Albigna DN	A	19.8	4
Hintereis F. DN	B	23.0	34
Hohlaub-N UP	A	26.5	5
Antizana 15a DN	C	27.0	-
Brewster DN	B	29.0	38
Silvretta DN	A	35.4	6
Forno DN	A	38.6	6
Storbreen DN	C	57.0	-
Hohlaub-N DN	A	57.3	39
Tschierva DN	B	58.0	26
Arolla (Bas) DN	B	70.0	35
Chamberlin DN	C	81.0	-
Valsorey DN	B	82.0	38
Djankuat DN	C	93.0	-
Tsidjore Nouve DN	B	122.0	-

8 References

Discharge estimations



Appendix 6 Hydrograph of the modelled specific discharge of Chamberlin Glacier (GL). In the time period 2010 – 2016, the modelled discharges have increased significantly compared to the values of the years 1980 – 2009. Chamberlin Glacier serves as one example, but similar modelling results have been observed for the majority of the 20 glaciers.

B. Results

*Summary of all the regression inputs**Appendix 7 Resulting values of the glaciological variables for the upper and lower sampling sites of the studied 20 glaciers.*

ID	Glacier name	Site	Surface Area [km ²]	Glacier coverage [%]	Gl. Index	Snout dist. [m]	years since ice-free	Q _{abs} S. month [km ³ /m]	CV of Q _{abs}
13	Brewster	UP	1.68 +- 0.06	0.52 +- 0.02	0.99	18	7	0.0017	0.90
		DN	1.68 +- 0.06	0.45 +- 0.02	0.84	241	29	0.0017	0.90
22	Valsorey	UP	1.97 +- 0.19	0.43 +- 0.04	0.95	76	7	0.0011	1.00
		DN	2.04 +- 0.19	0.25 +- 0.02	0.60	963	82	0.0011	1.00
25	Findelen	UP	15.38 +- 0.32	0.75 +- 0.02	0.96	158	5	0.0094	0.96
		DN	15.38 +- 0.32	0.73 +- 0.02	0.86	651	16	0.0094	0.96
27	Arolla (Bas)	UP	4.77 +- 0	0.78 +- 0	0.95	125	6	0.0027	1.02
		DN	10.43 +- 0.2	0.4 +- 0.01	0.71	1328	70	0.0059	1.03
28	Tsidjore	UP	2.77 +- 0.05	0.6 +- 0.01	0.96	76	11	0.0014	0.99
		DN	2.77 +- 0.05	0.58 +- 0.01	0.76	534	122	0.0014	0.99
29	Mont Mine	UP	10.48 +- 0.1	0.64 +- 0.01	0.99	35	2	0.0059	1.11
		DN	10.48 +- 0.1	0.62 +- 0.01	0.86	547	18	0.0059	1.11
30	Hohlaub-N	UP	0.33 +- 0	0.64 +- 0.01	0.74	205	27	0.0002	0.94
		DN	0.33 +- 0	0.63 +- 0.01	0.63	343	57	0.0002	0.94
31	Schwarzberg	UP	5.84 +- 0.23	0.72 +- 0.03	0.97	72	9	0.0051	0.89
		DN	5.84 +- 0.23	0.68 +- 0.03	0.92	200	18	0.0051	0.89
39	Chamberlin	UP	4.21 +- 0	0.94 +- 0	0.98	40	1	0.0024	0.88
		DN	4.35 +- 0.03	0.74 +- 0.01	0.62	1306	81	0.0024	0.88
48	Djankuat	UP	2.57 +- 0.18	0.71 +- 0.05	1.00	3	0	0.0017	0.77
		DN	2.91 +- 0.2	0.32 +- 0.02	0.62	1049	93	0.0035	0.77
67	Antizana 15a	UP	0.29 +- 0	0.81 +- 0.01	0.78	156	19	0.0001	0.51
		DN	0.29 +- 0	0.69 +- 0.01	0.56	418	27	0.0001	0.51
76	Trift VS	UP	1.55 +- 0.08	0.67 +- 0.03	0.97	33	2	0.0014	0.92
		DN	1.55 +- 0.08	0.64 +- 0.03	0.78	357	15	0.0014	0.92
77	Forno	UP	5.98 +- 0.27	0.44 +- 0.02	0.99	31	2	0.0061	0.91
		DN	6.1 +- 0.27	0.38 +- 0.02	0.73	907	39	0.0061	0.91
78	Albigna	UP	2.6 +- 0.09	0.37 +- 0.01	0.97	58	5	0.0025	0.88
		DN	2.64 +- 0.09	0.36 +- 0.01	0.86	267	20	0.0025	0.88
79	Morteratsch	UP	15.77 +- 0.2	0.62 +- 0.01	1.00	2	1	0.0155	1.07
		DN	15.77 +- 0.21	0.61 +- 0.01	0.92	334	4	0.0155	1.07
80	Roseg	UP	3.34 +- 0.06	0.75 +- 0.01	0.71	119	5	0.0034	1.05
		DN	3.78 +- 0.12	0.54 +- 0.02	0.84	796	13	0.0034	1.05
81	Tschierva	UP	6.11 +- 0.1	0.6 +- 0.01	0.97	69	3	0.0064	0.96
		DN	6.11 +- 0.1	0.55 +- 0.01	0.64	1402	56	0.0064	0.96
82	Silvretta	UP	2.36 +- 0.06	0.66 +- 0.02	0.96	61	6	0.0022	0.90
		DN	2.36 +- 0.06	0.61 +- 0.02	0.83	309	35	0.0022	0.90
83	Hintereis F.	UP	7.79 +- 0.59	0.49 +- 0.04	0.89	331	10	0.0079	0.97
		DN	7.88 +- 0.62	0.44 +- 0.03	0.76	905	23	0.0079	0.97
94	Storbreen	UP	2.7 +- 0.08	0.8 +- 0.02	0.94	20	3	0.0026	0.89
		DN	2.7 +- 0.08	0.78 +- 0.02	0.99	306	57	0.0026	0.89

8 References

Appendix 8 Measured values of the physicochemical stream variables and chlorophyll a concentration.

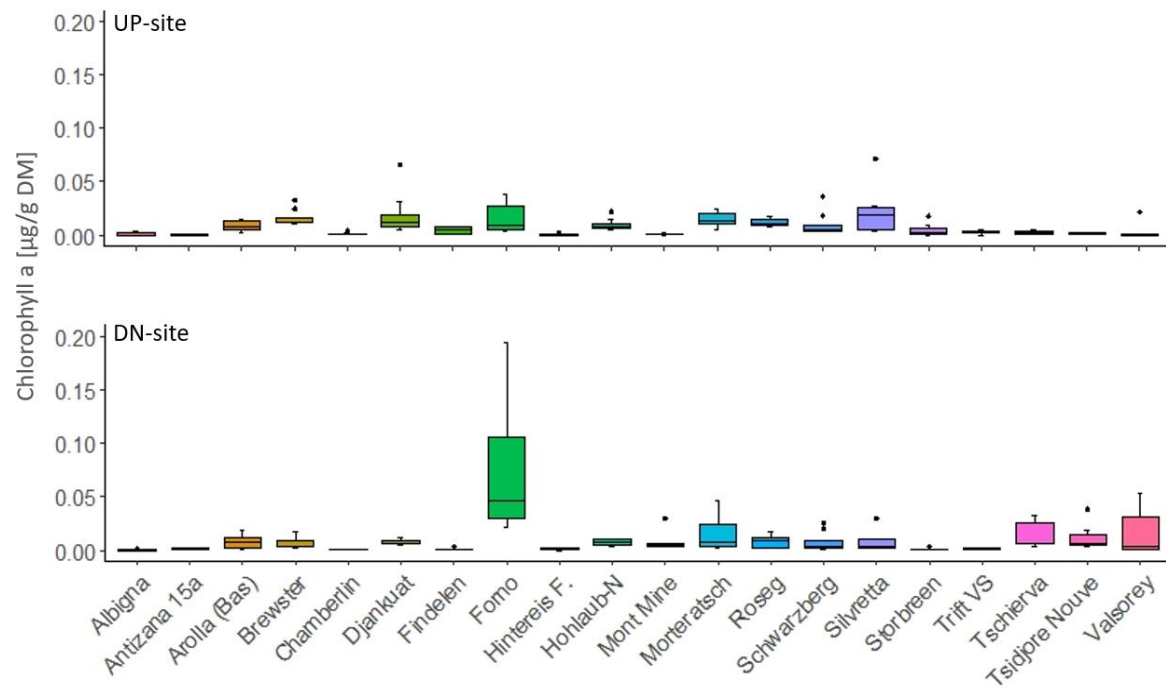
ID	Glacier name	Site	Temperature [°C]	Conductivity [µS/cm]	Turbidity [NTU]	Chl a [µg Chl a/g DM]
13	Brewster	UP	0.7	9.3	5.0	0.0172
		DN	0.9	6.9	4.5	0.0083
22	Valsorey	UP	0.2	120.3	235.3	0.0026
		DN	4.7	163.0	140.3	0.0155
25	Findelen	UP	0.5	158.0	111.3	0.0047
		DN	0.7	163.9	136.3	0.0011
27	Arolla (Bas)	UP	0.3	53.7	90.6	0.0088
		DN	3.1	74.6	1048.0	0.0084
28	Tsidjore Nouve	UP	0.0	173.0	79.2	0.0012
		DN	2.1	160.2	72.8	0.0116
29	Mont Mine	UP	0.6	47.7	132.7	0.0010
		DN	1.7	44.5	131.7	0.0072
30	Hohlaub-N	UP	4.8	207.0	11.0	0.0093
		DN	2.8	189.0	8.8	0.0076
31	Schwarzberg	UP	0.4	64.3	206.0	0.0100
		DN	1.8	73.0	132.7	0.0080
39	Chamberlin	UP	0.2	5.3	90.8	0.0015
		DN	2.3	7.7	228.3	0.0005
48	Djankuat	UP	1.0	76.3	9.2	0.0188
		DN	3.9	75.9	233.7	0.0080
67	Antizana 15a	UP	5.5	3.6	493.7	0.0003
		DN	5.0	3.5	532.7	0.0013
76	Trift VS	UP	1.1	75.2	34.2	0.0030
		DN	2.4	59.5	71.0	0.0016
77	Forno	UP	1.8	15.2	129.3	0.0150
		DN	7.9	32.5	83.0	0.0775
78	Albigna	UP	0.3	14.1	369.7	0.0010
		DN	1.4	12.8	223.3	0.0002
79	Morteratsch	UP	0.1	4.2	198.7	0.0143
		DN	3.3	4.2	102.2	0.0160
80	Roseg	UP	3.2	17.4	9.7	0.0121
		DN	5.8	19.9	7.1	0.0084
81	Tschierva	UP	0.8	34.8	70.8	0.0023
		DN	4.8	30.8	132.7	0.0136
82	Silvretta	UP	1.0	25.1	55.9	0.0221
		DN	0.8	23.9	70.0	0.0077
83	Hintereis F.	UP	0.5	94.3	390.3	0.0006
		DN	1.7	84.9	286.0	0.0008
94	Storbreen	UP	0.6	9.9	79.6	0.0044
		DN	0.6	5.3	26.0	0.0010

Appendix 9 Information on the sampled glaciers, locations of the sampling points and the day of sampling.

ID	Glacier name	Polit. Unit	WGMS-ID	Site	Latitude	Longitude	Altitude	Sampling date
13	Brewster	NZ	1597	UP	61.5818	169.4317	1699	2/13/2019
				DN	61.5841	169.4305	1655	2/13/2019
22	Valsorey	CH	365	UP	46.8169	7.2669	2441	6/25/2019
				DN	46.8199	7.2570	2387	6/25/2019
25	Findelen	CH	389	UP	46.8559	7.8263	2557	6/7/2020
				DN	46.8545	7.8199	2508	6/7/2020
27	Arolla (Bas)	CH	377	UP	46.4035	7.4960	2265	6/8/2020
				DN	46.4122	7.4921	2112	6/8/2020
28	Tsidjore Nouve	CH	376	UP	46.3850	7.4692	2277	6/9/2020
				DN	46.3909	7.4736	2148	6/9/2020
29	Mont Mine	CH	378	UP	46.4197	7.5505	2085	6/11/2020
				DN	46.4227	7.5535	1977	6/11/2020
30	Hohlaub-N	CH	5434	UP	46.3131	7.9939	3081	6/30/2020
				DN	46.3151	7.9921	2983	6/30/2020
31	Schwarzberg	CH	395	UP	46.3352	7.9390	2662	7/1/2020
				DN	46.3431	7.9397	2659	7/1/2020
39	Chamberlin	GL	3735	UP	46.1358	-53.5282	468	7/19/2019
				DN	46.1361	-53.4954	332	7/19/2019
48	Djankuat	RU	726	UP	-0.4739	42.7501	2760	9/19/2019
				DN	-0.4718	42.7396	2640	9/19/2019
67	Antizana 15a	EC	1624	UP	43.2034	-78.1543	4828	2/15/2020
				DN	43.2088	-78.1555	4782	2/15/2020
76	Trift VS	CH	5435	UP	69.3204	7.9866	2868	7/2/2020
				DN	69.3210	7.9823	2788	7/2/2020
77	Forno	CH	396	UP	46.0265	9.7018	2254	7/4/2020
				DN	46.0276	9.7006	2223	7/4/2020
78	Albigna	CH	1674	UP	46.1446	9.6464	2176	7/5/2020
				DN	46.1449	9.6468	2165	7/5/2020
79	Morteratsch	CH	1673	UP	46.0396	9.9338	2176	7/6/2020
				DN	46.0437	9.9335	2063	7/6/2020
80	Roseg	CH	406	UP	46.0160	9.8419	2276	7/7/2020
				DN	46.0188	9.8443	2161	7/7/2020
81	Tschierva	CH	405	UP	45.9901	9.8695	2326	7/8/2020
				DN	46.0006	9.8576	2098	7/8/2020
82	Silvretta	CH	408	UP	46.0108	10.0569	2474	7/10/2020
				DN	46.0105	10.0542	2430	7/10/2020
83	Hintereis F.	AT	491	UP	45.9166	10.7994	2489	7/12/2020
				DN	45.9208	10.8056	2410	7/12/2020
94	Storbreen	NO	302	UP	-44.0819	8.1625	1441	8/24/2020
				DN	-44.0838	8.1654	1365	8/24/2020

8 References

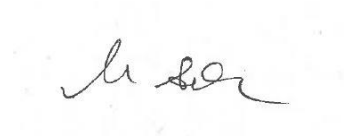
Observed chlorophyll a concentrations



Appendix 10 Inter- and intra-site distribution of observed chlorophyll a values. Extremely high chlorophyll a concentrations were observed at the lower sampling site of Forno Glacier (CH).

Personal Declaration

I hereby declare that the submitted thesis is the result of my own, independent work. All external sources are explicitly acknowledged in the thesis.

A handwritten signature in black ink, appearing to read 'Martina Schön', is written on a light-colored, slightly textured background.

Martina Schön

Lausanne, 30.06.21